



Flares in Sgr A* from GRMHD Simulations

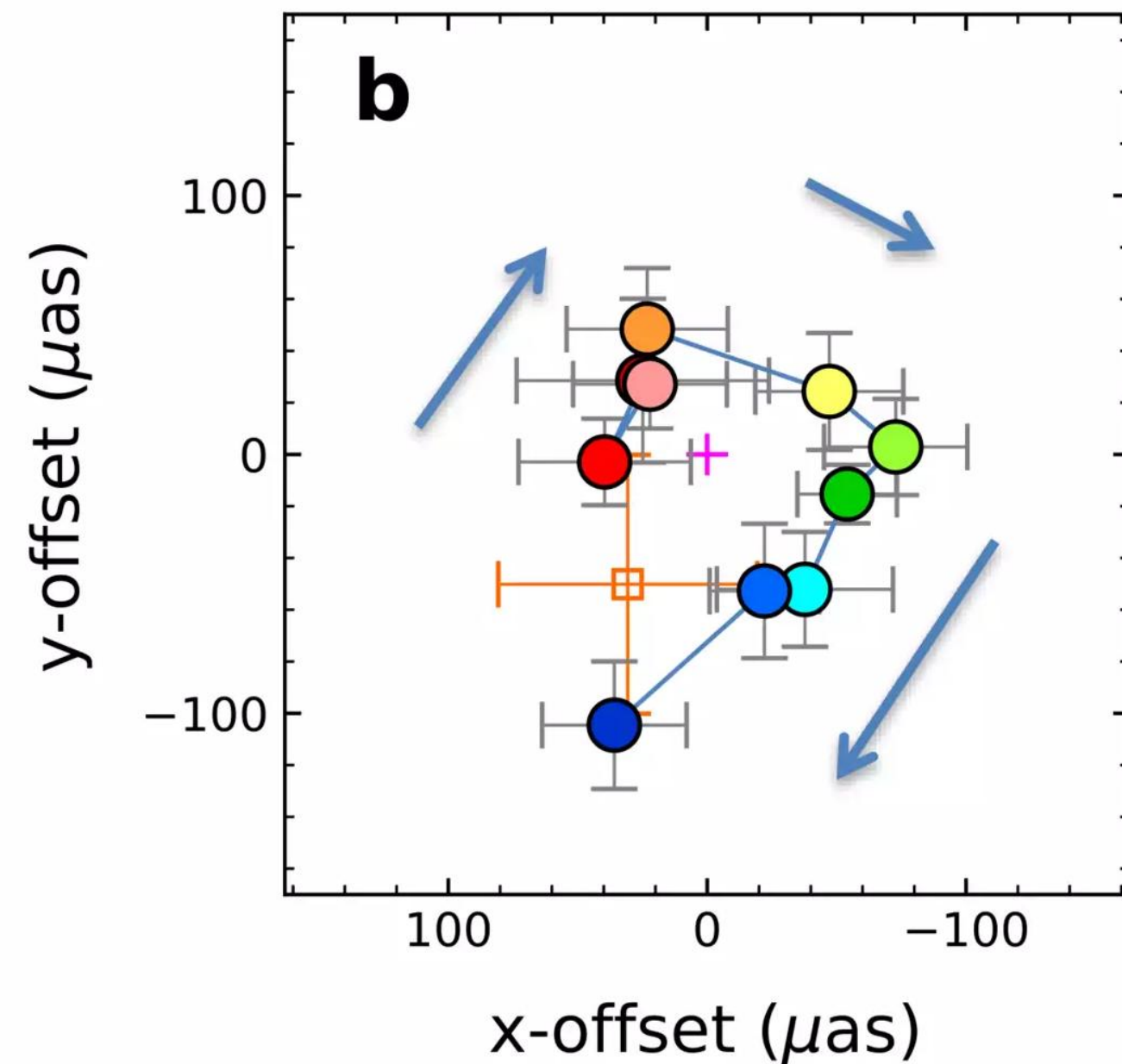
Yosuke Mizuno

Tsung-Dao Lee Institute, Shanghai Jiao Tong University

Table of Contents

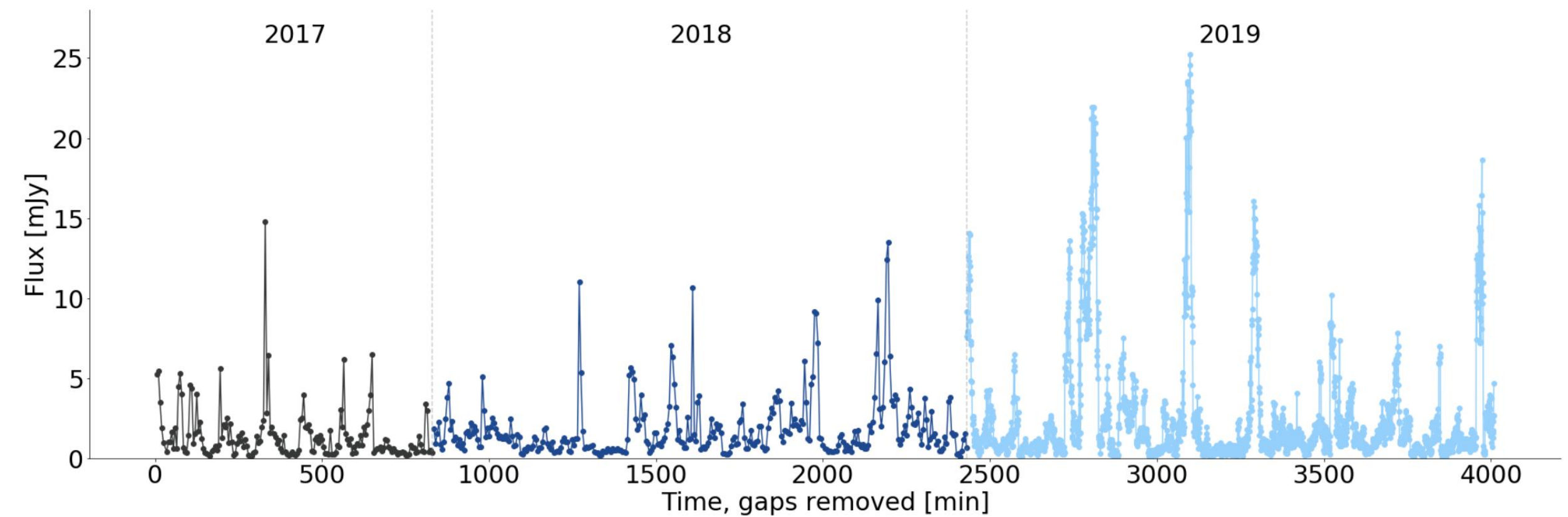
- Introduction of relativistic jet and EHT collaboration
- Theoretical modeling for black hole shadow and jet
- M87 jet modeling
- Particle acceleration (mechanism & site) in relativistic jets
- Summary

Flares from Sgr A*

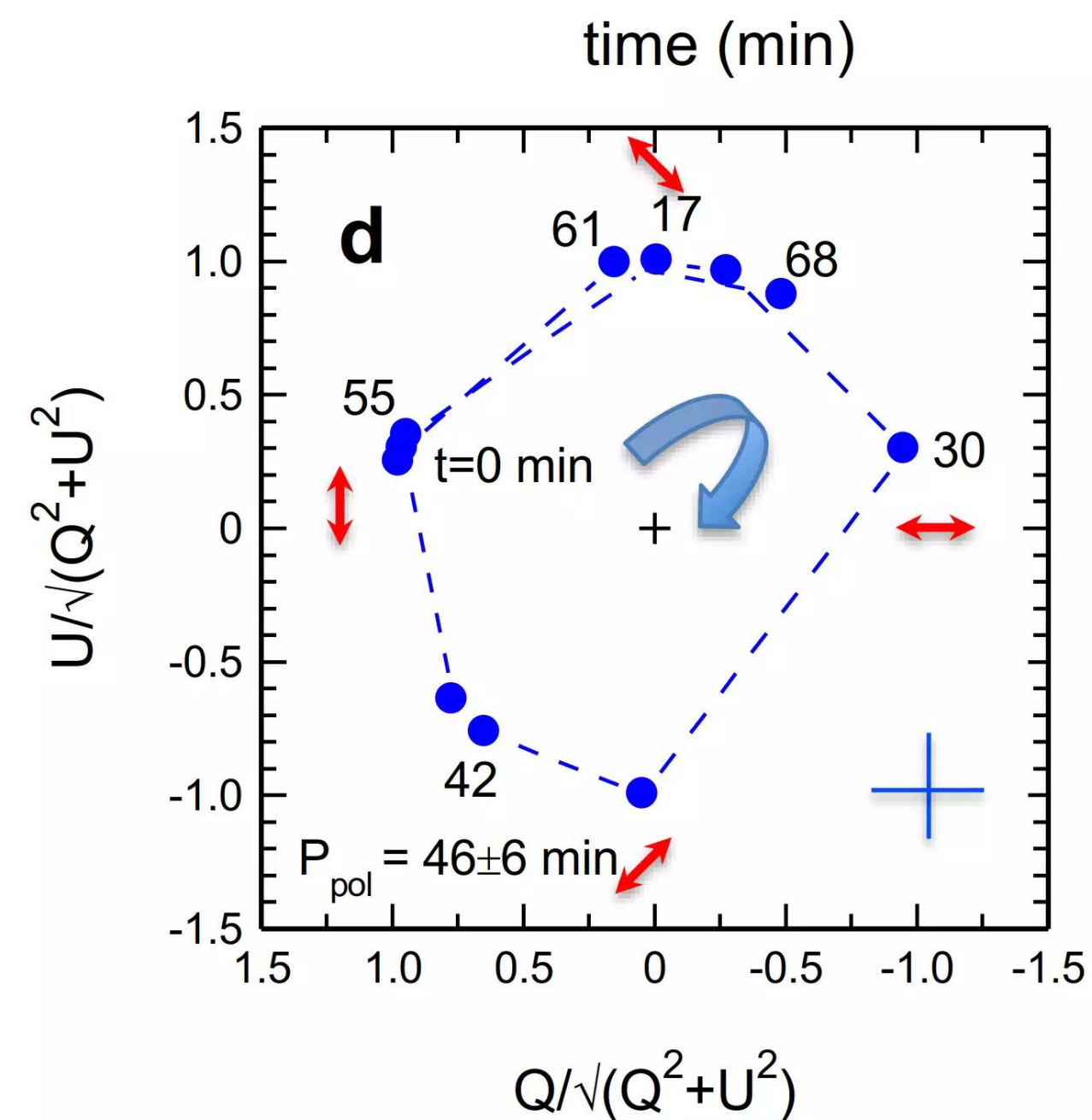


GRAVITY collaboration et al. (2018)

Orbital motions of gas swirling at about 30% of light speed near the black hole ($\sim 7 r_g$).



NIR flux distribution from Abuter et al. (2020)

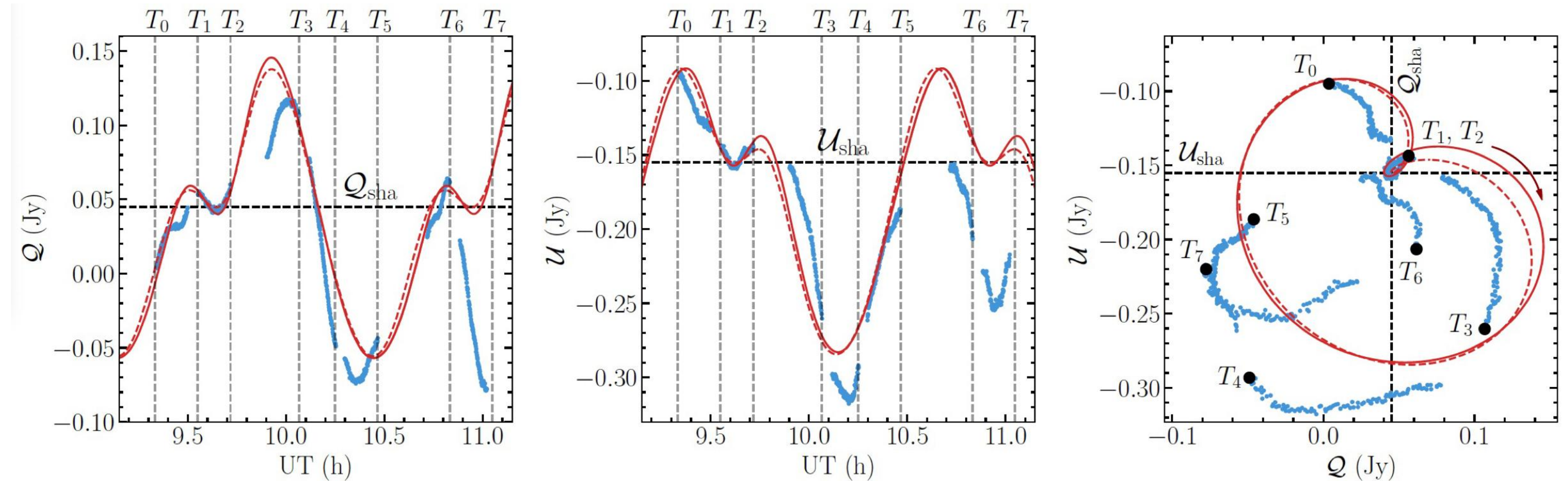


Polarization change (field rotation) on QU plane during the NIR flare

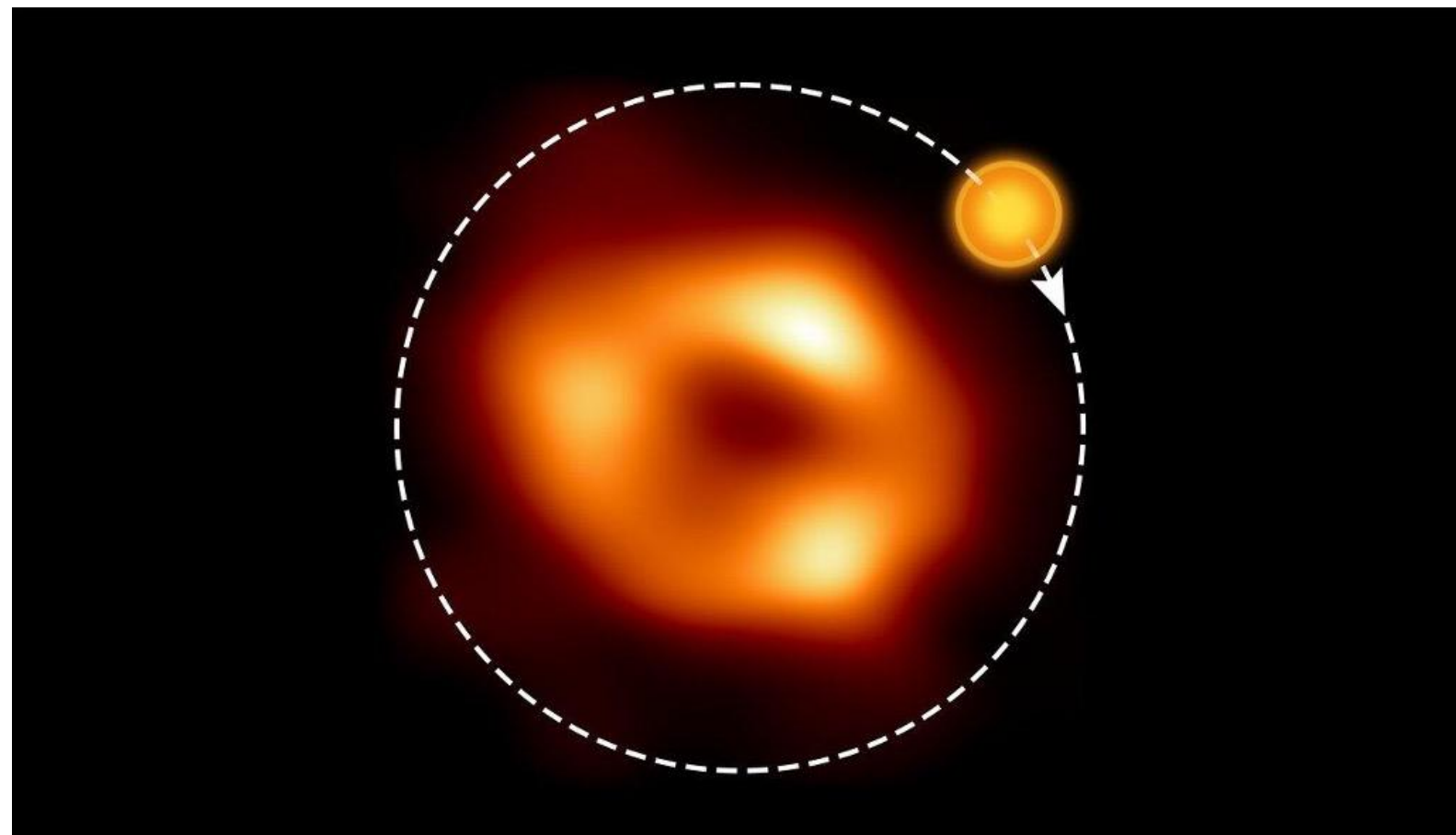
Frank's talk

Flares from Sgr A*

- Orbital motion in (mm) radio light curves during the Sgr A* flare
- Polarization change (field rotation) on QU plane during the flare
- The semi-analytic orbiting hot spot model is well explained observed QU loop



Wielgus et al. (2022), Vos et al (2022)



What is the origin of hot spot?

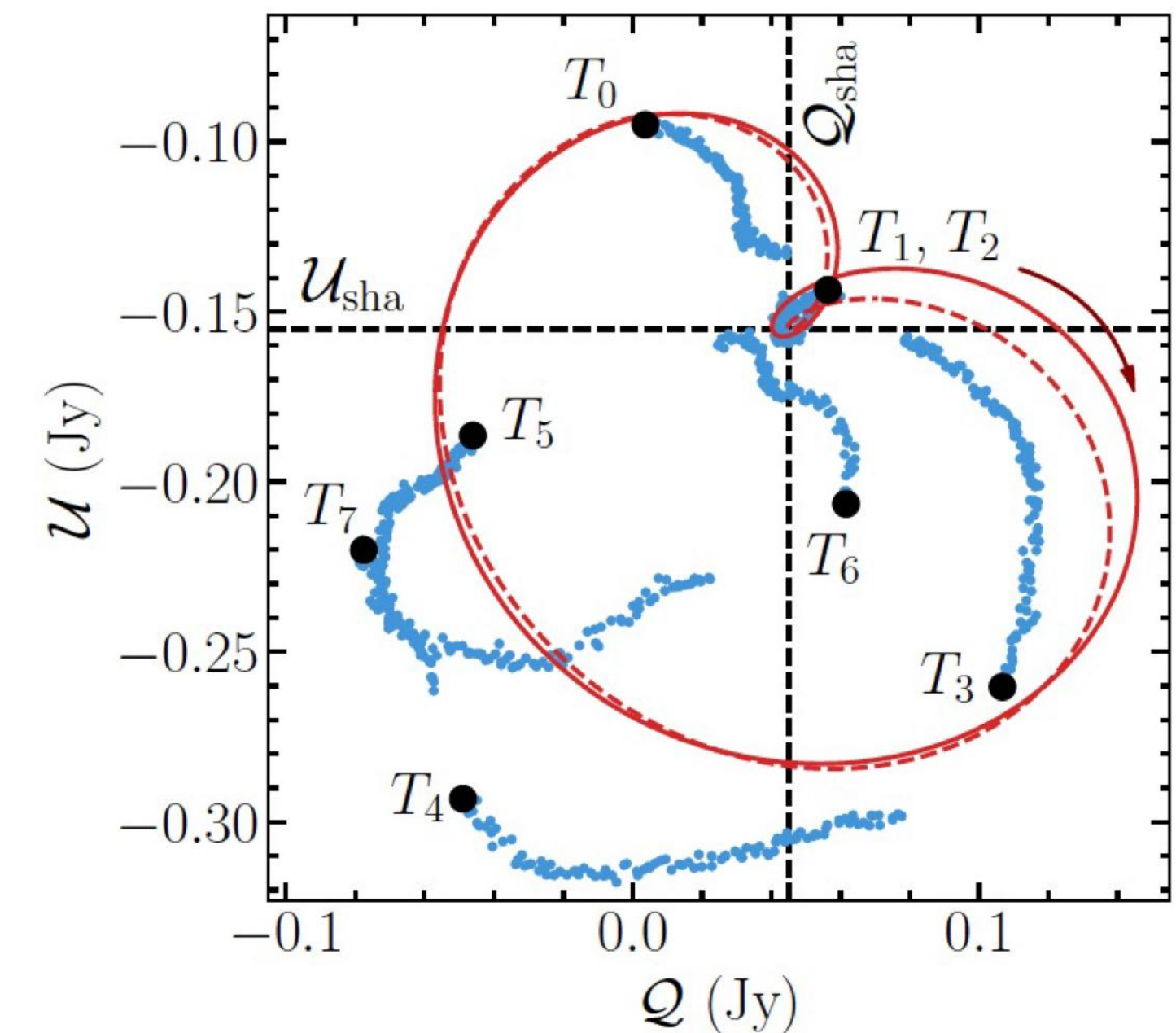
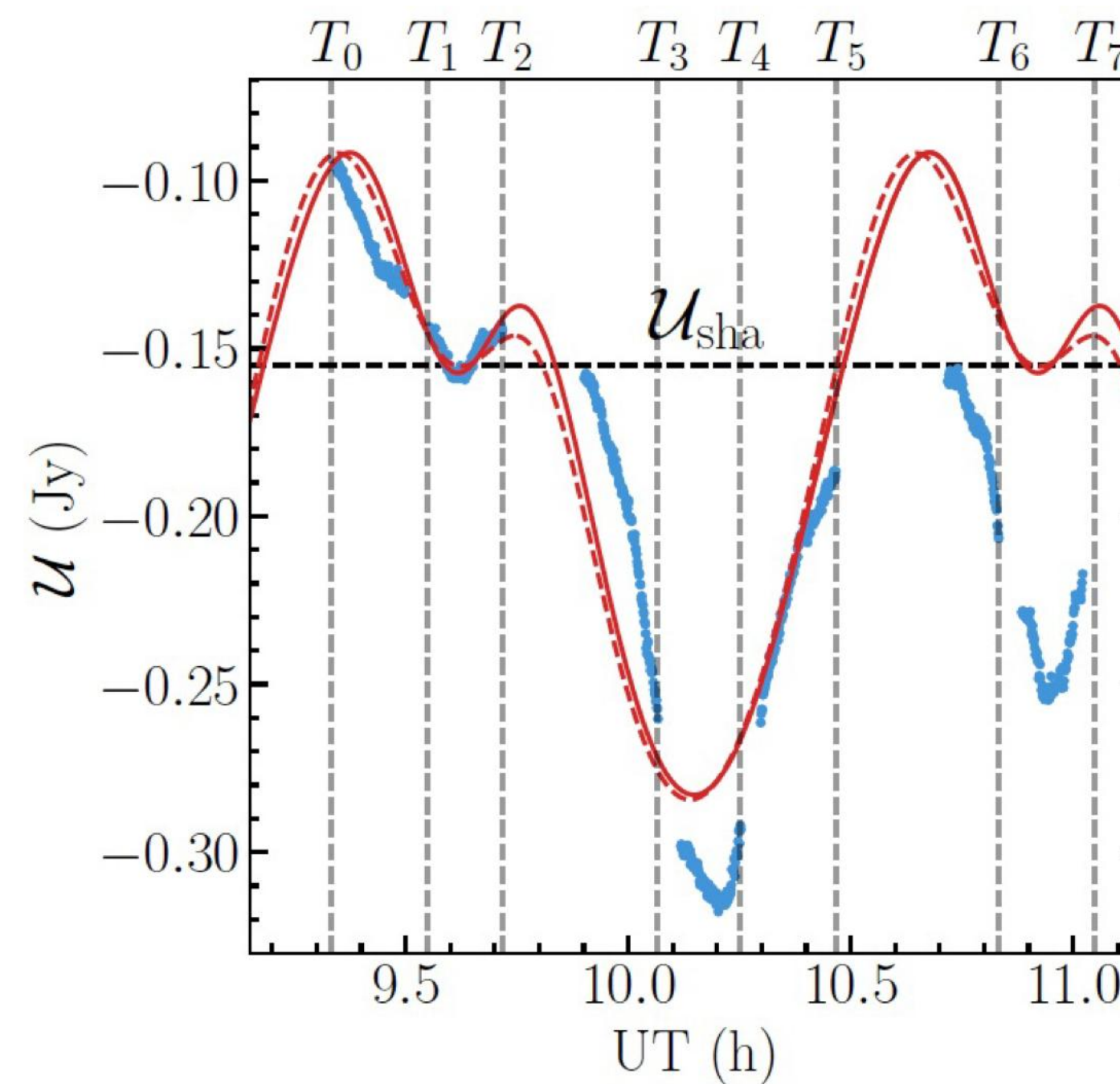
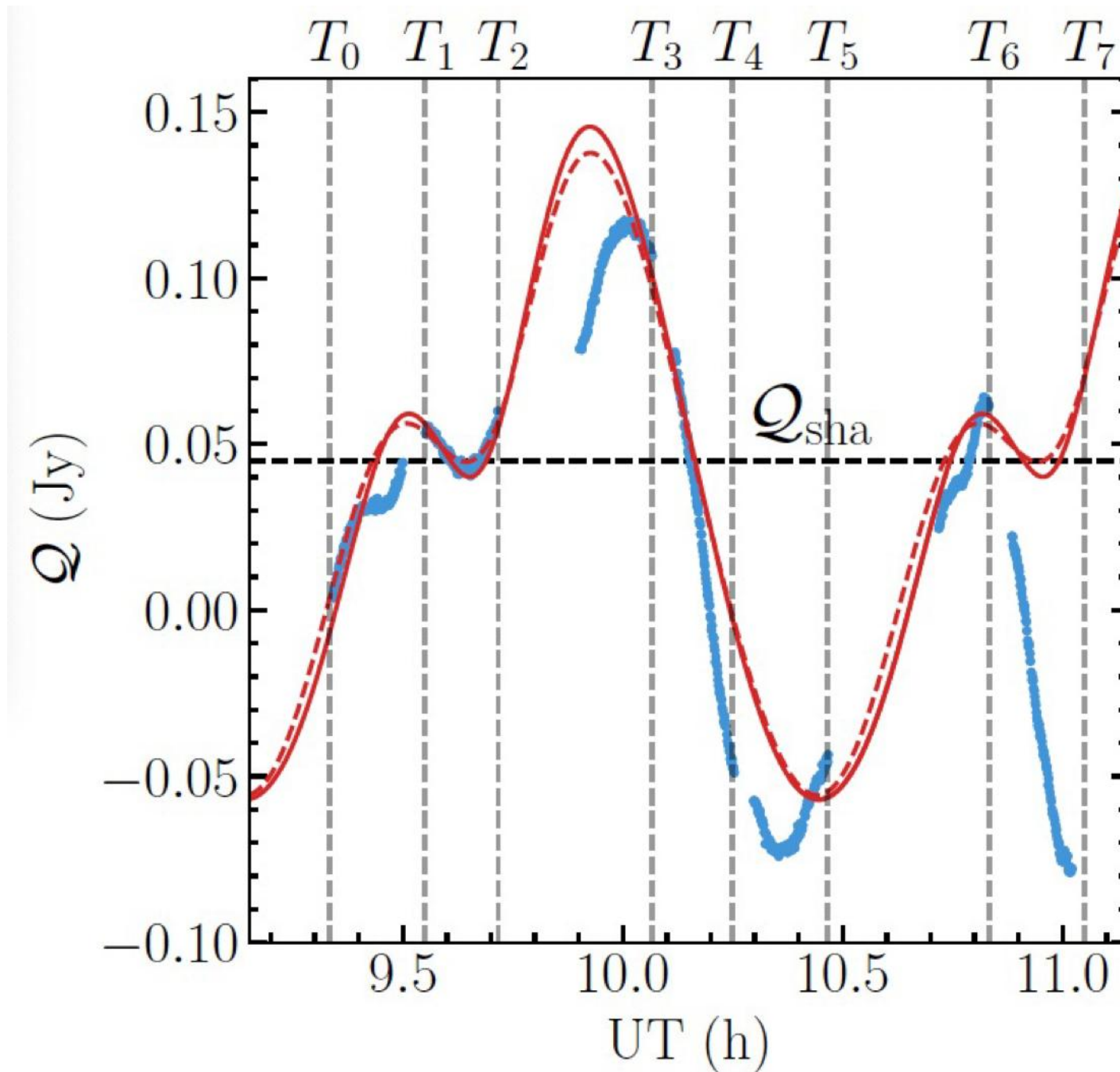
- Magnetic bundle eruption on equatorial plane from MAD
- Flux eruptions or plasmoid chain in jet sheath

Flares from Sgr A*

- A similar QU-loop pattern is also observed from sub-mm radio frequency after X-ray flare
- Semi-analytic orbiting hot-spot model on the equatorial plane can explain QU-loop structure ($R \sim 11 r_g$ at $i = 158^\circ$)

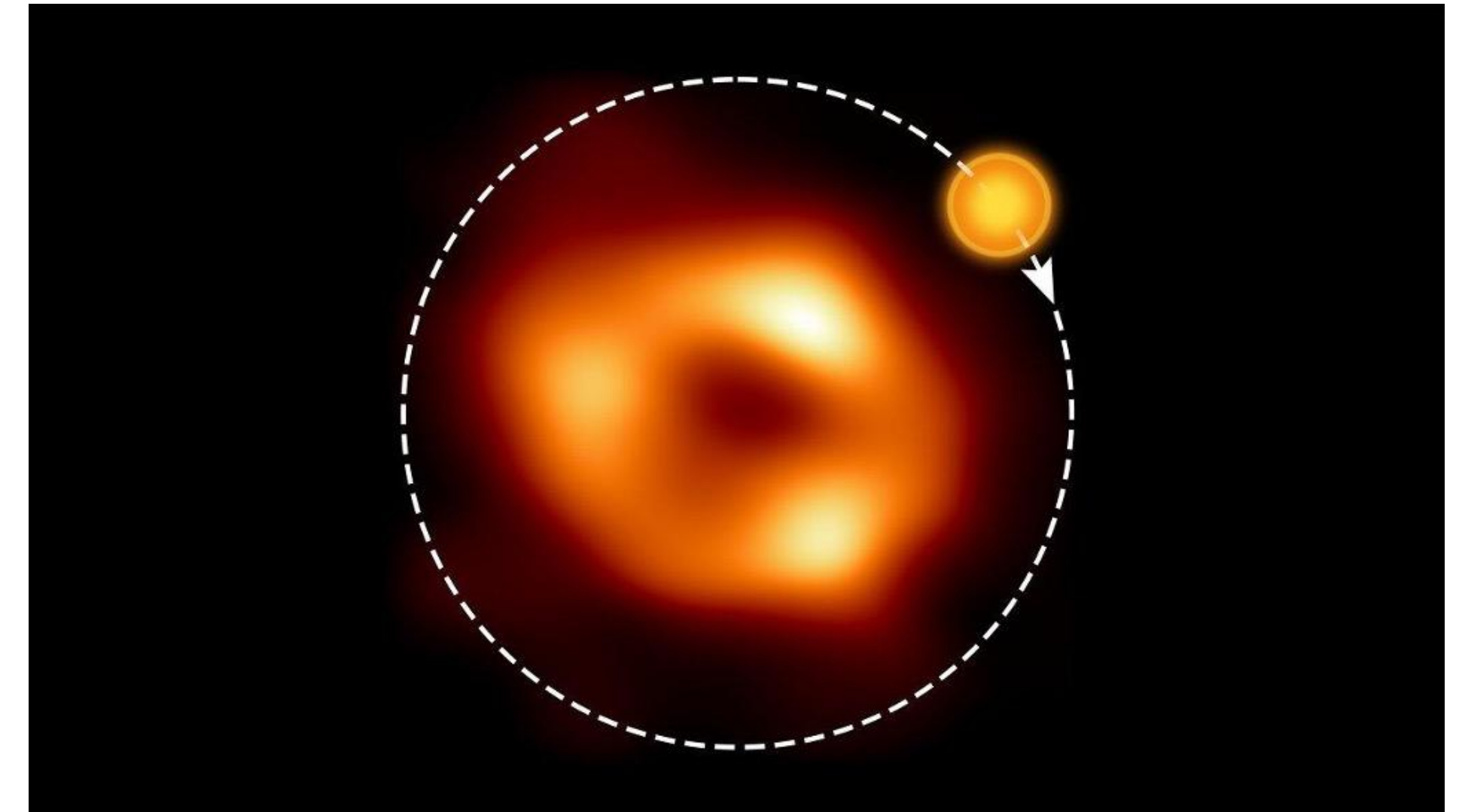
sub-mm

ALMA observations (Wiegus et al. 2022, Vos et al. 2022)



Hot-spot in Sgr A*

- A semi-analytic hot spot model can explain orbiting motion and polarized QU loop pattern seen in NIR and sub-mm observation during Sgr A* flare
- Q: What is the origin of hot-spot?
 - Magnetic bundle eruption on an equatorial plane from MAD accretion flows
 - Flux eruptions or plasmoid chains in jet sheath



EHT Sgr A* Observations

$$M_{\text{BH}} \sim 4 \times 10^6 M_{\odot}$$

$$\dot{M} \sim (5.2 - 9.5) \times 10^{-9} M_{\odot} \text{yr}^{-1} i \leq 30^{\circ}$$

- Ring-like emission comes from the accretion flow or jet base
- Theoretical best-bet model prefers MAD with a lower inclination angle (<30 degrees) and higher BH spin

Sgr A*



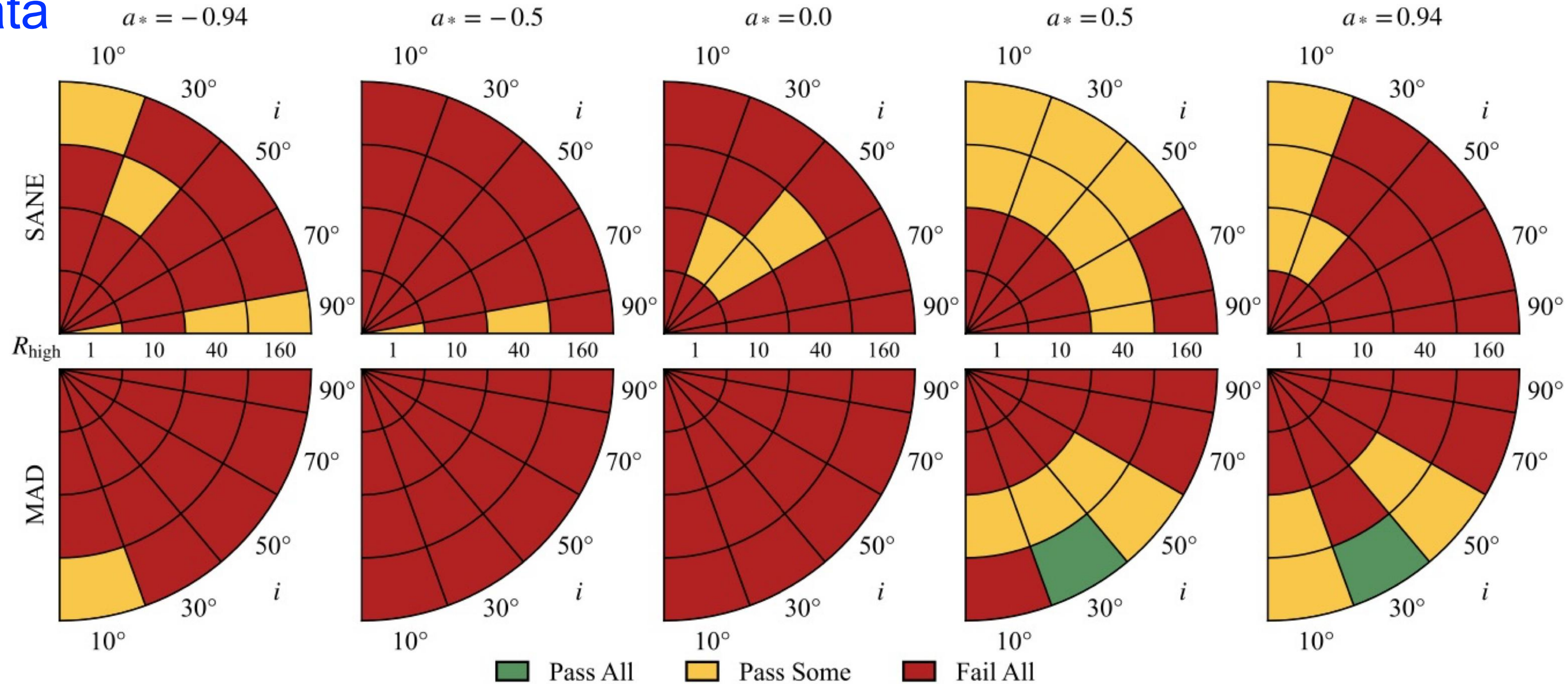
Observational Constraints (Sgr A*)

- **Three classes of constraints:** EHT, non-EHT, and variability
- **EHT (5 constraints):** image size (second moment); visibility amplitude morphology; m-ring diameter, width, and asymmetry
- **non-EHT (4 constraints):** 86 GHz flux density & image size, 2 μ m flux density, X-ray 2-10keV luminosity
- **Variability (2 constraints):** 1.3mm lightcurve variability on 3hr intervals (moderation Index), light-curve normalized visibility amplitude variability at ~ 4 G λ

constraint
230 GHz size
VA morphology
M-ring diameter
M-ring width
M-ring asym.
86 GHz flux
86 GHz size
2.2 μ m flux
X-ray flux
lc variability
4 G λ variability

Combined data constraints without variability (fiducial model)

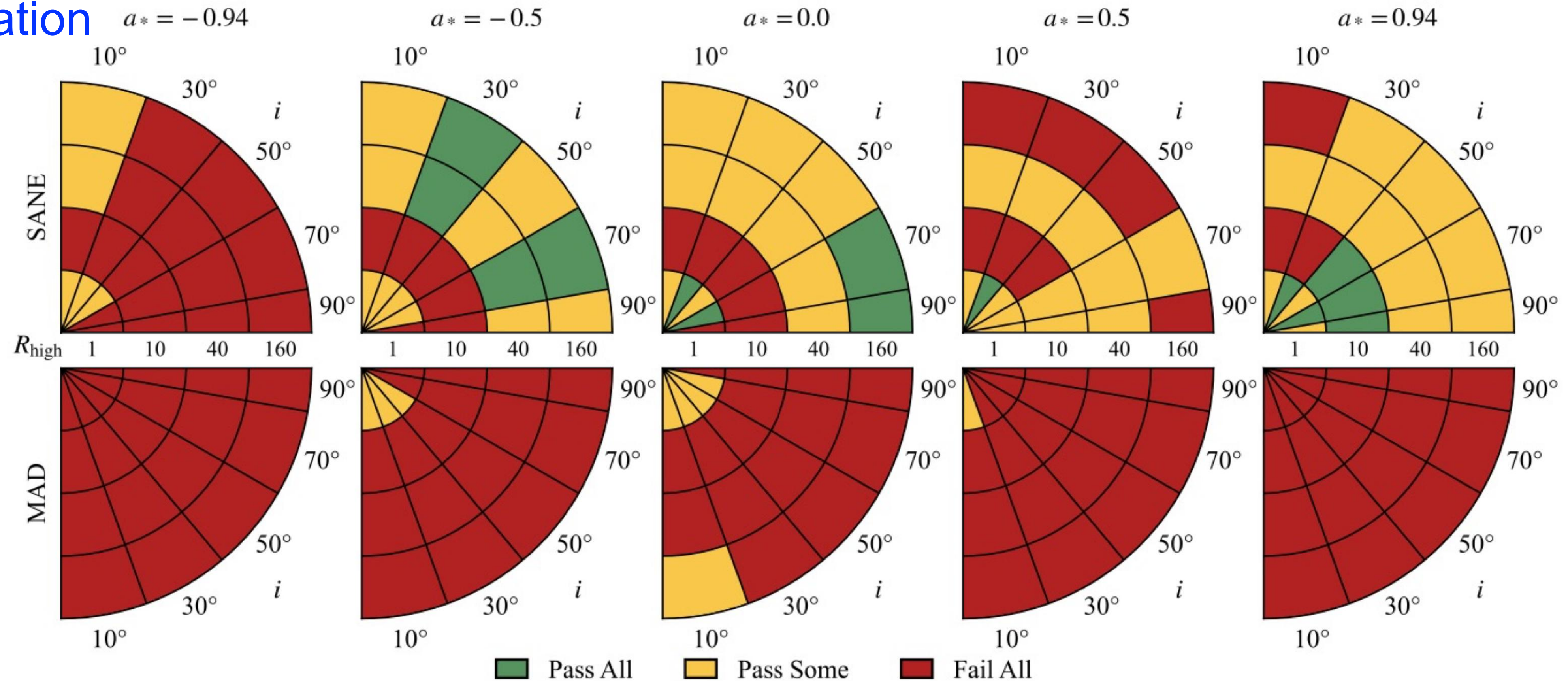
EHT+non-EHT data
(w.o. variability)



- A number of models fail only the variability constraints.
- A promising cluster of passed models: MAD with inclination $i \leq 30$ deg (interestingly no SANE model survive)

Data constraints by variability (fiducial model)

*M₃: 3-hour modulation
index (~ 530M)
[variability]



- Light curve variability provides a particularly severe *constraint*, failing nearly all MAD models and a large fraction of SANE models = *best-bet model is failed*.

EHT Sgr A* Polarimetry

- Emission ring is highly polarized
- EVPA shows a helically twisted pattern
- peak fractional polarization of $\sim 40\%$
- Circular polarization: 5~10%
- If RM is attributed to external Faraday screen \Rightarrow derotation of EVPA ~ 46 deg.

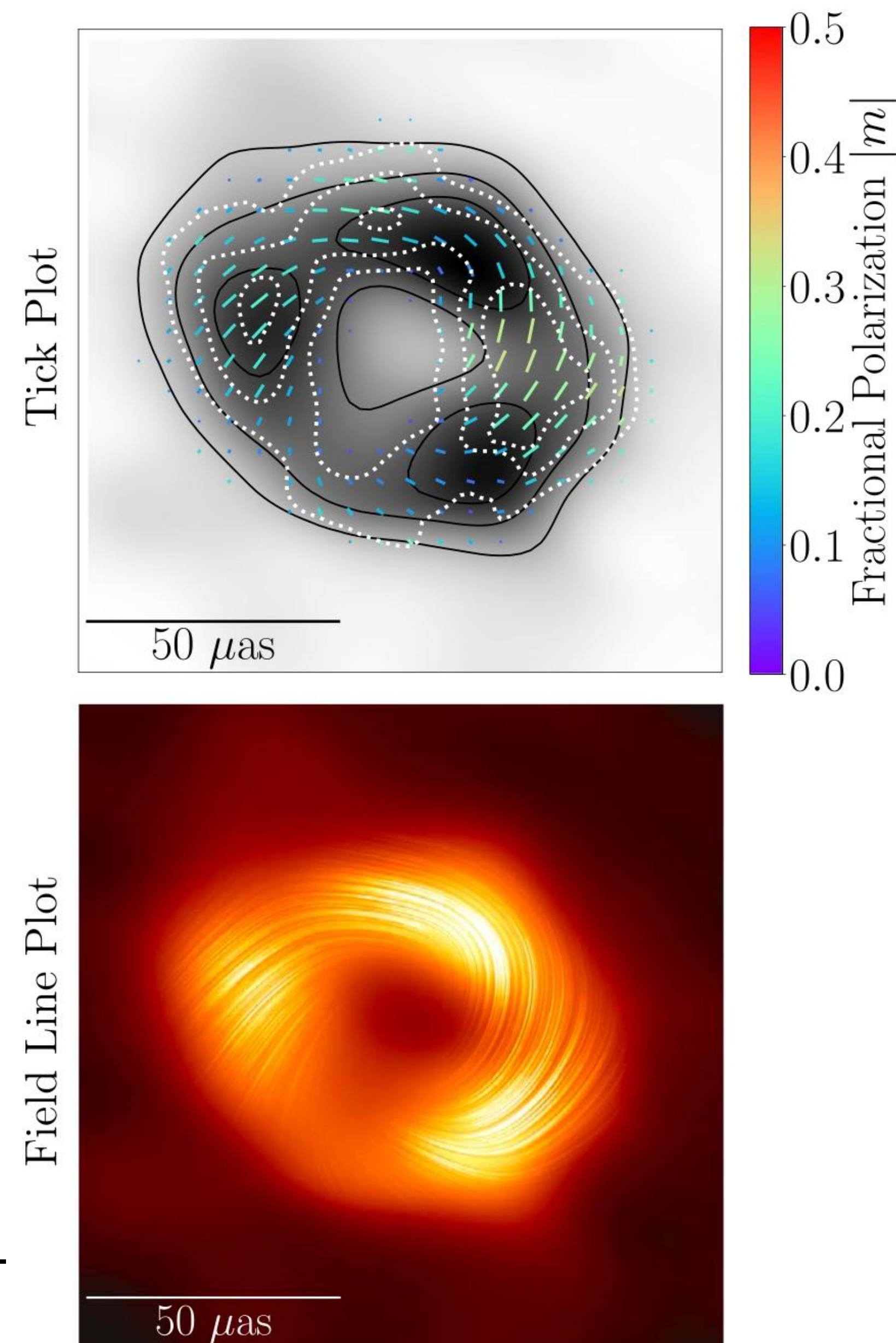


Image-Averaged Quantities

net linear polarization fraction

$$|m|_{\text{net}} = \frac{\sqrt{(\sum_i Q_i)^2 + (\sum_i U_i)^2}}{\sum_i I_i} \quad v_{\text{net}} = \frac{\sum_i V_i}{\sum_i I_i}$$

intensity-weighted average polarization fraction

$$\langle |m| \rangle = \frac{\sum_i \sqrt{Q_i^2 + U_i^2}}{\sum_i I_i} \quad \langle |v| \rangle = \frac{\sum_i |V_i|/I_i I_i}{\sum_i I_i}$$

polarization structure with a decomposition into azimuthal mode (Palumbo et al. 20)

$$\beta_2 = \frac{1}{I_{\text{ring}}} \int_{\rho_{\text{min}}}^{\rho_{\text{max}}} \int_0^{2\pi} P(\rho, \varphi) e^{-2i\varphi} \rho d\varphi d\rho$$

Table 6
Polarimetric Constraints Derived from the Primary Methods THEMIS and Snapshot m-ring Modeling

Observable	Snapshot m-ring	THEMIS	Combined
$ m_{\text{net}} $ (%)	(2.0, 3.1)	(6.5, 7.3)	(2.0, 7.3)
v_{net} (%)	...	(−0.7, 0.12)	(−0.7, 0.12)
$\langle m \rangle$ (%)	(24, 28)	(26, 28)	(24, 28)
$\langle v \rangle$ (%)	(1.4, 1.8)	(2.7, 5.5)	(0.0, 5.5)
$ \beta_1 $	(0.11, 0.14)	(0.10, 0.13)	(0.10, 0.14)
$ \beta_2 $	(0.20, 0.24)	(0.14, 0.17)	(0.14, 0.24)
$\angle\beta_2$ (deg) (as observed)	(125, 137)	(142, 159)	(125, 159)
$\angle\beta_2$ (deg) (RM derotated)	(−168, −108)	(−151, −85)	(−168, −85)
$ \beta_2 / \beta_1 $	(1.5, 2.1)	(1.1, 1.6)	(1.1, 2.1)

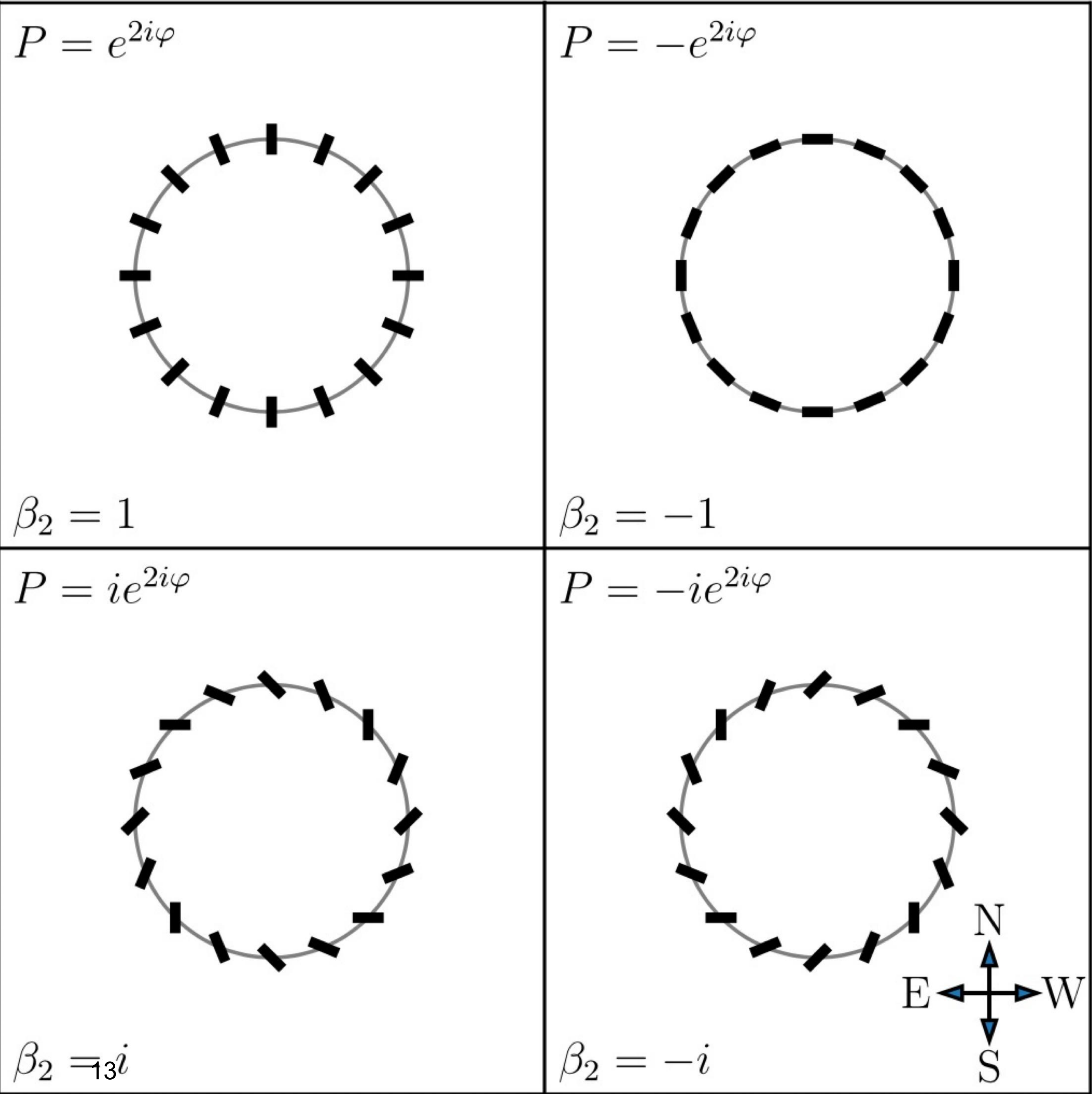
Azimuthal mode of Polarized Structure

Expand a linearly polarized image from multipole series in polar coordinates (ρ , φ):

$$\beta_2 = \frac{1}{I_{\text{ring}}} \int_{\rho_{\text{min}}}^{\rho_{\text{max}}} \int_0^{2\pi} P(\rho, \varphi) e^{-2i\varphi} \rho d\varphi d\rho$$

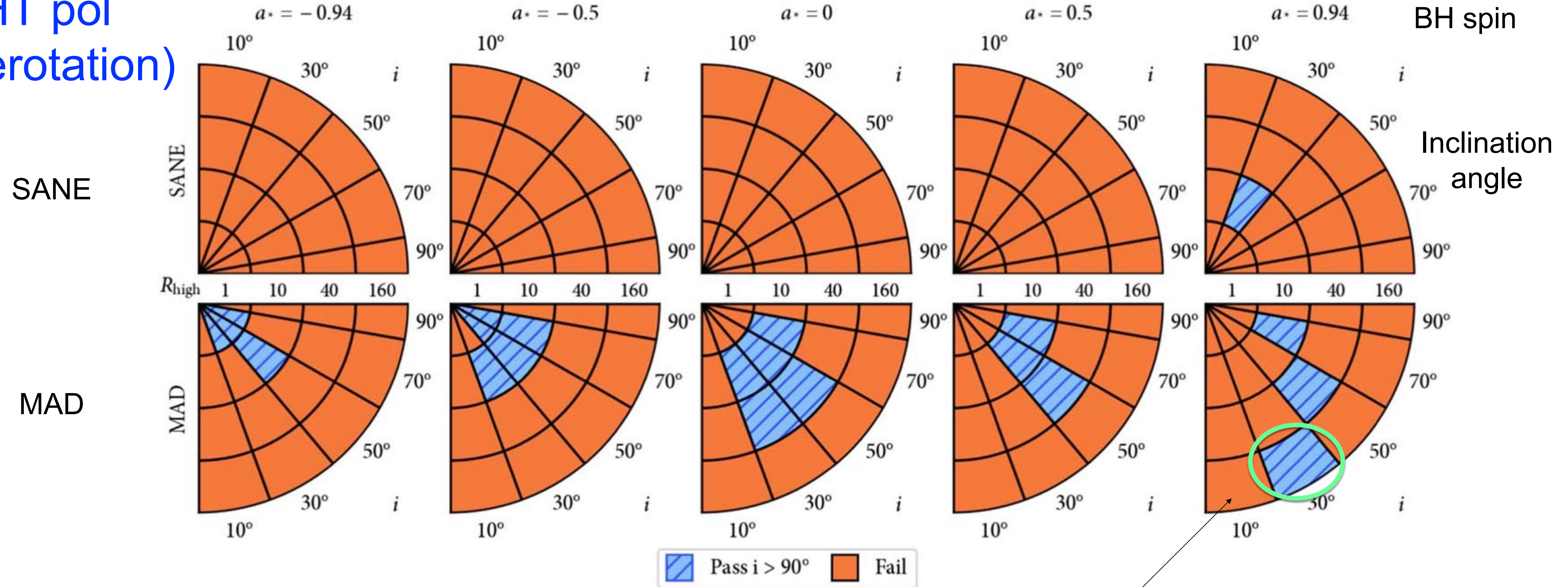
β_2 value (m=2 mode) reflects EVPA pattern.

(Palumbo et al. 20)



Data Constraints from EHT Polarimetry

EHT pol
(w. derotation)

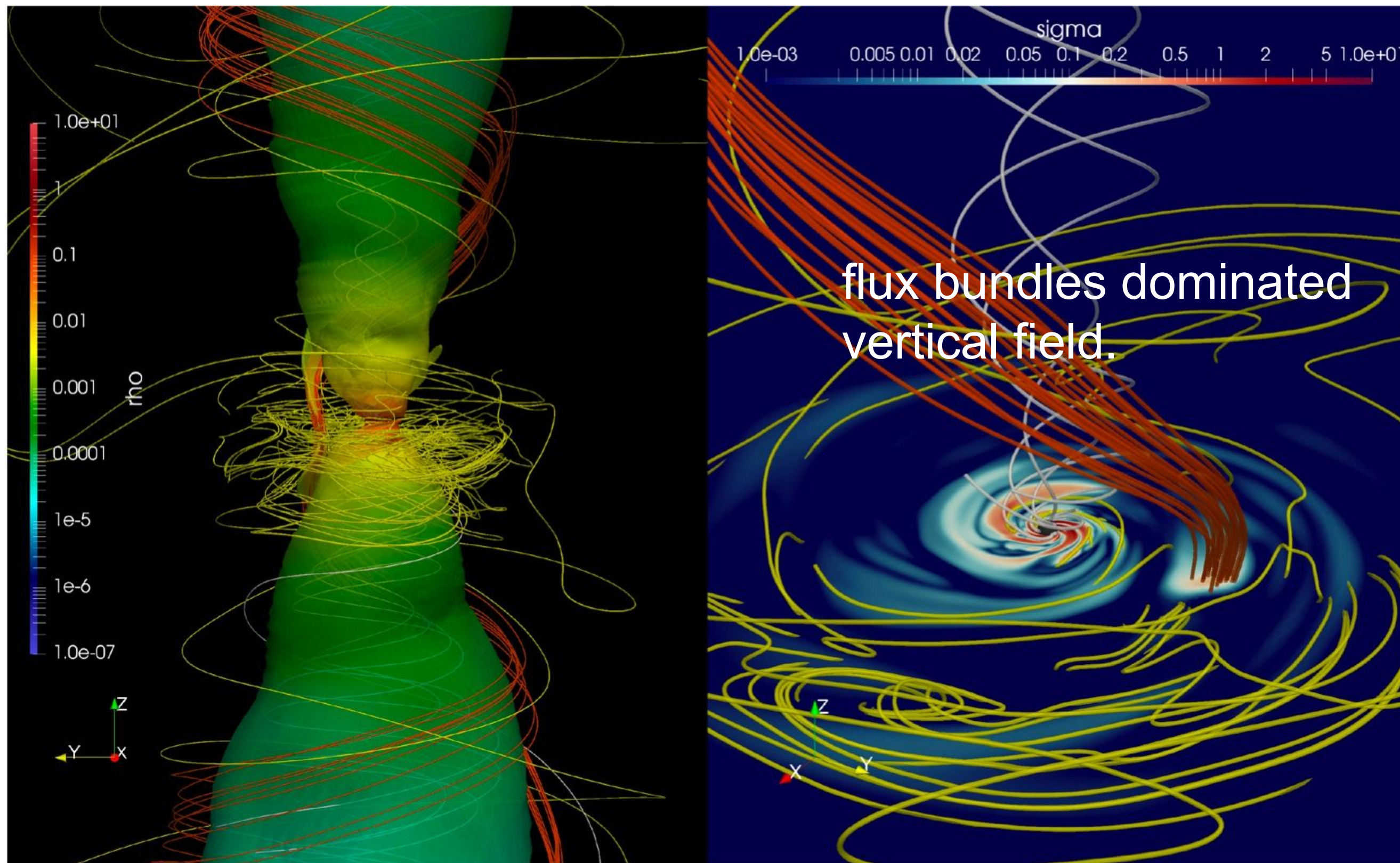


- Polarimetry gives strong constraints
- The best-bet **MAD model** from intensity modeling survived (MAD, $a=0.94$, $R_h=160$, $i=30$ deg)

1. Magnetized accretion flows with single magnetic loop

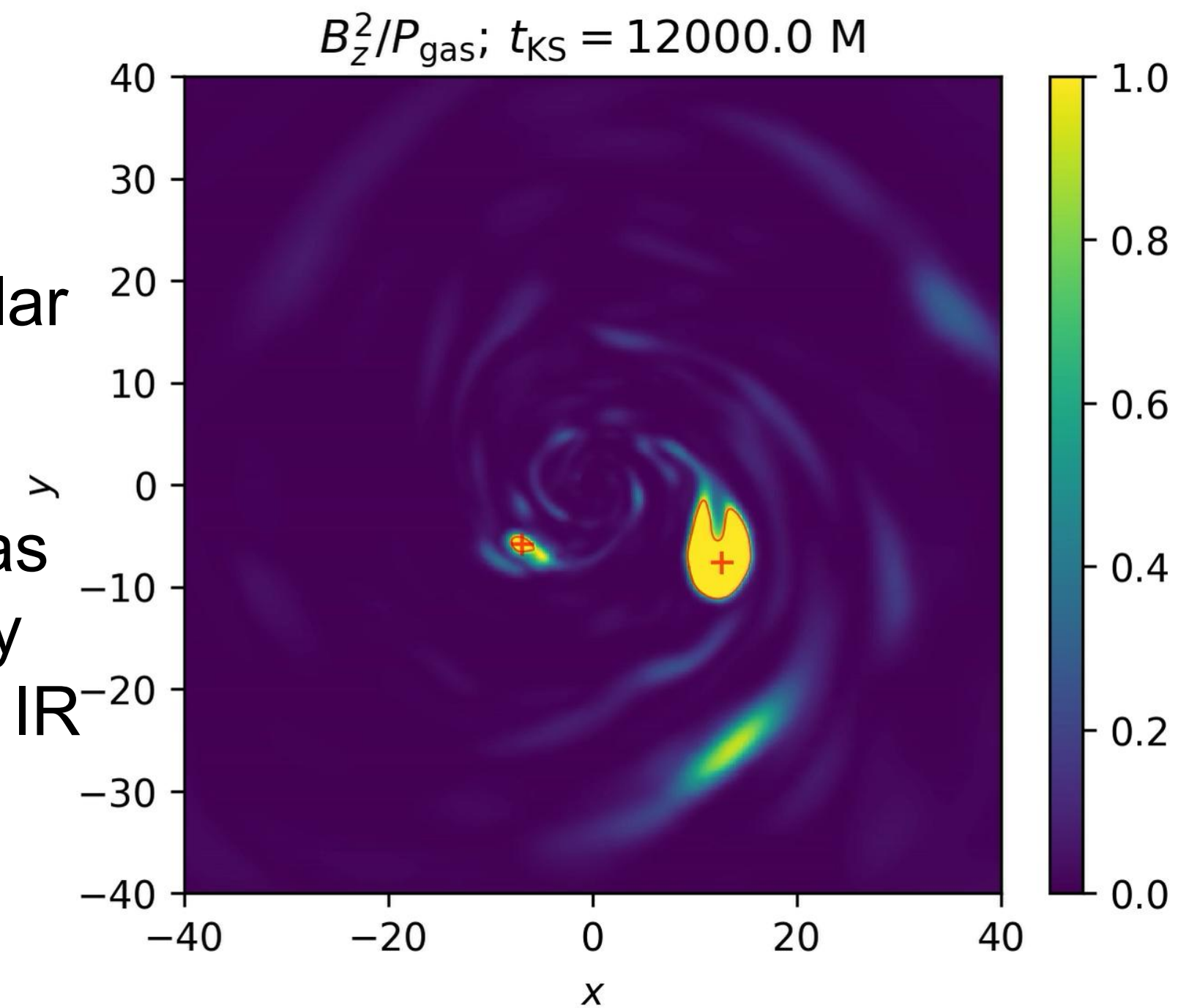
Porth, YM, Fromm (2021)
Najafi-Ziyazi, Davelaar, YM, Porth (2024)

Magnetic flux bundles from MAD



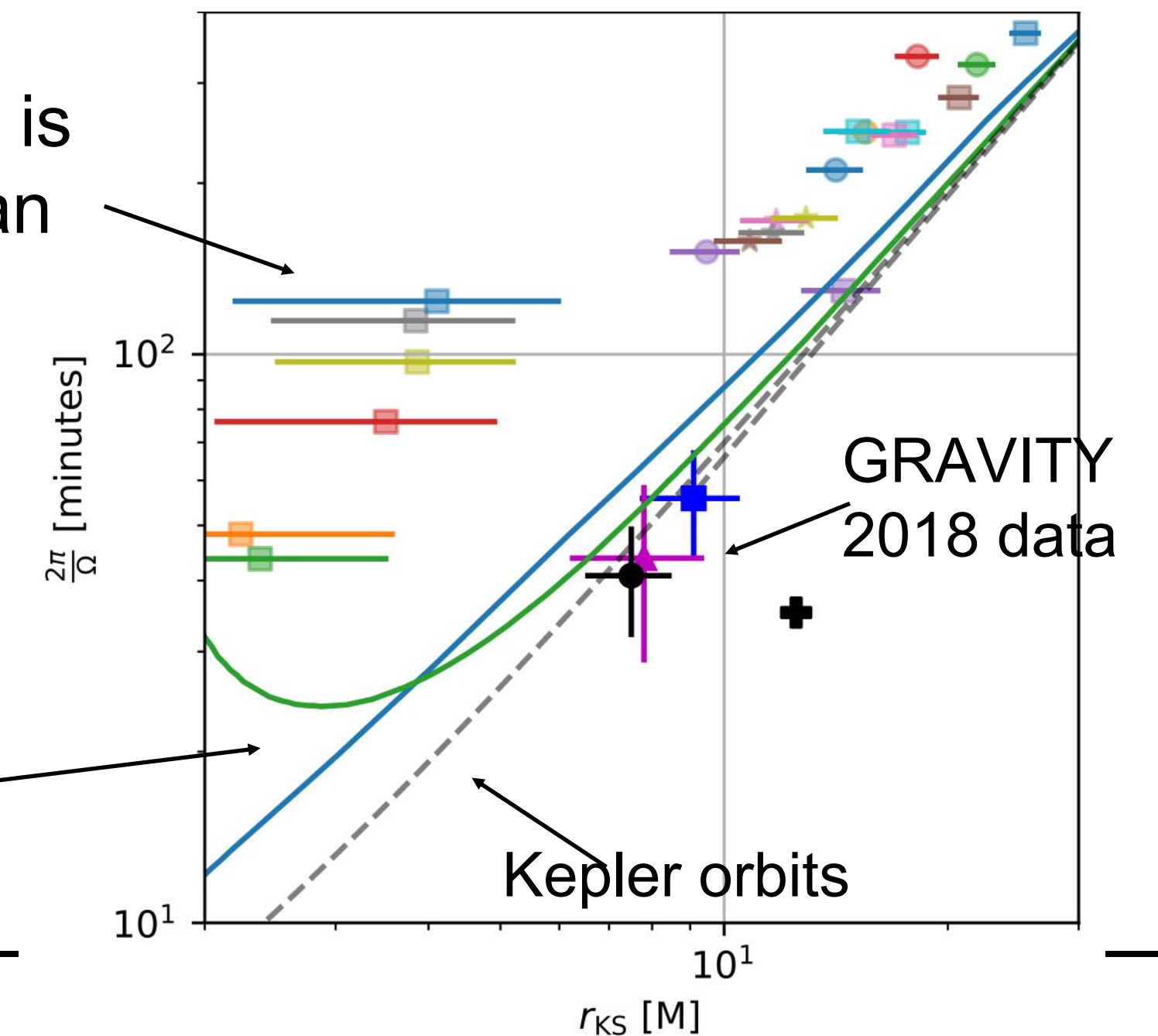
- SgrA* observation by GRAVITY shows traced IR flare at $\sim 10R_g$
- MAD shows violent episodes of flux escape via magnetic reconnection => Sgr A* flare?

- Tracking circular motion
- Flux bundle has enough energy ($\sim 10^{40}$ erg) for IR & X-ray flares



Pattern orbit is sub-Keplerian

Average rotation profiles



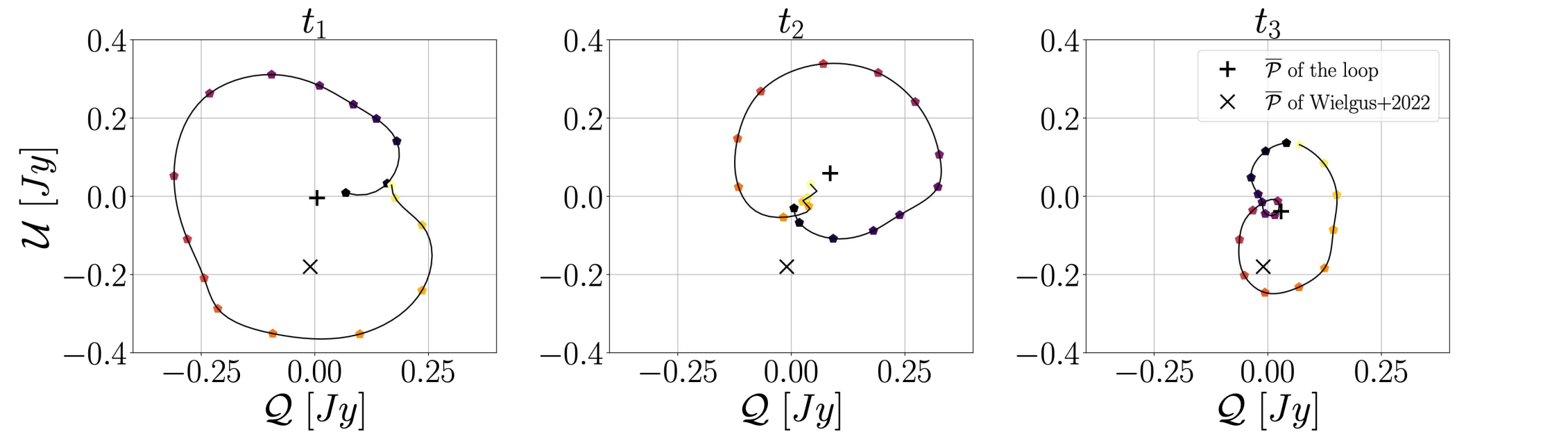
GRRT Calculation

- Using GRRT code RAPTOR for post-process imaging calculation
 - Target for Sgr A*
 - The accretion rate is fitted at 230 GHz with a flux of 2.5 Jy.
 - To avoid the floor value problem in GRMHD data, we cut-off a high magnetization region ($\sigma = 1$)
 - GRRT calculation uses the GRMHD data from 15,000 to 30,000 M
 - Consider thermal synchrotron emission
-

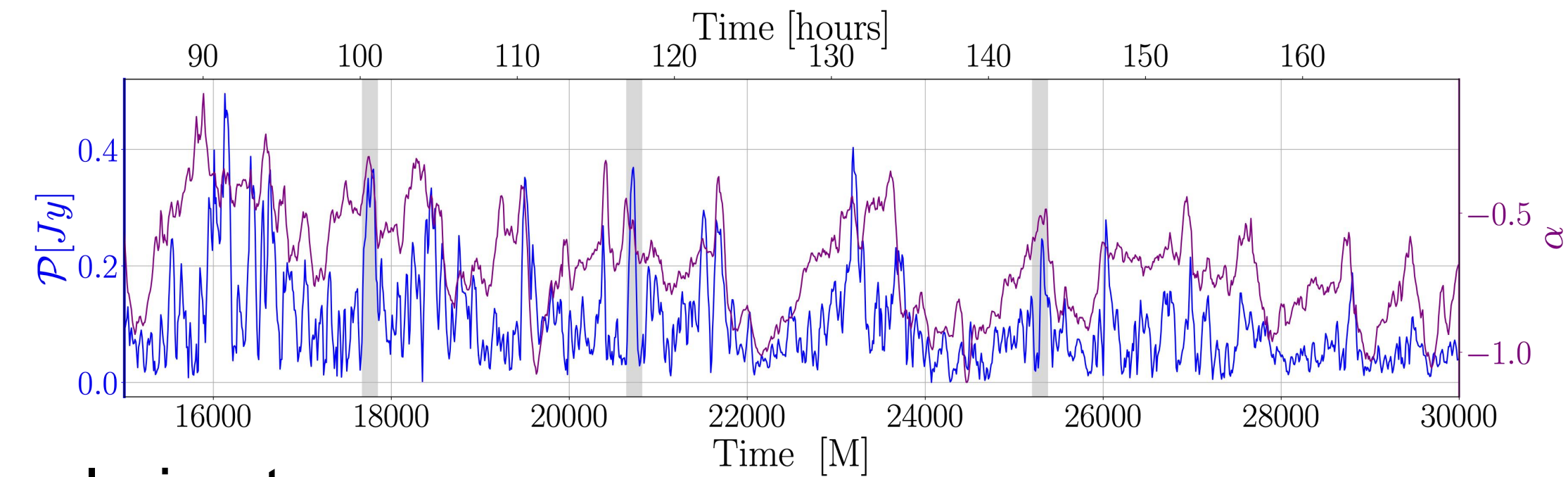
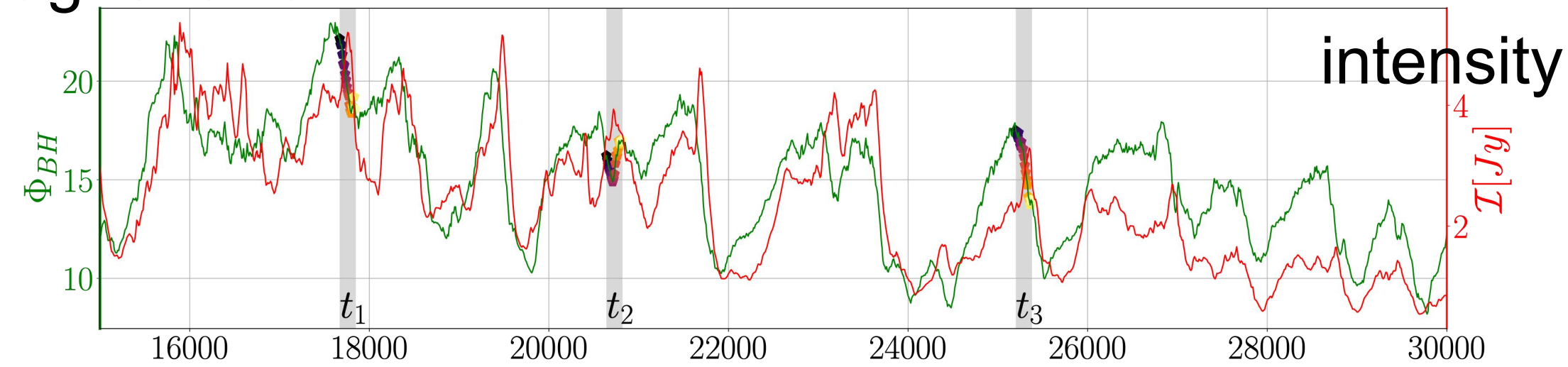
Sgr A* Flare from MAD

- During flare period, QU loop pattern is seen

@230GHz, MAD, $a=-0.94$, $i=10$ degree

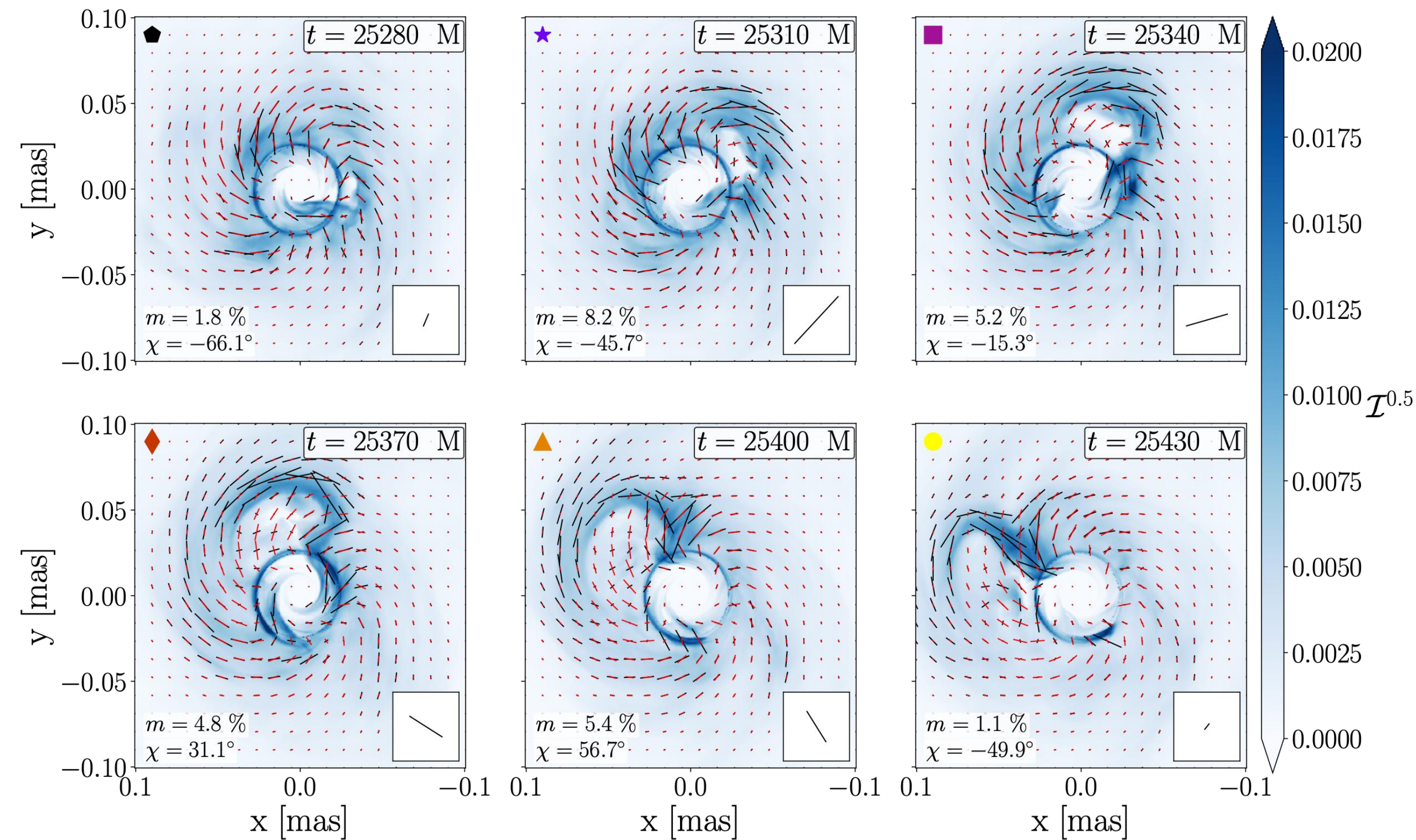


magnetic flux



polarimetry

intensity images with EVPA at t_3



2. Magnetized accretion flows with multiple magnetic loops



Hong-Xuan Jiang

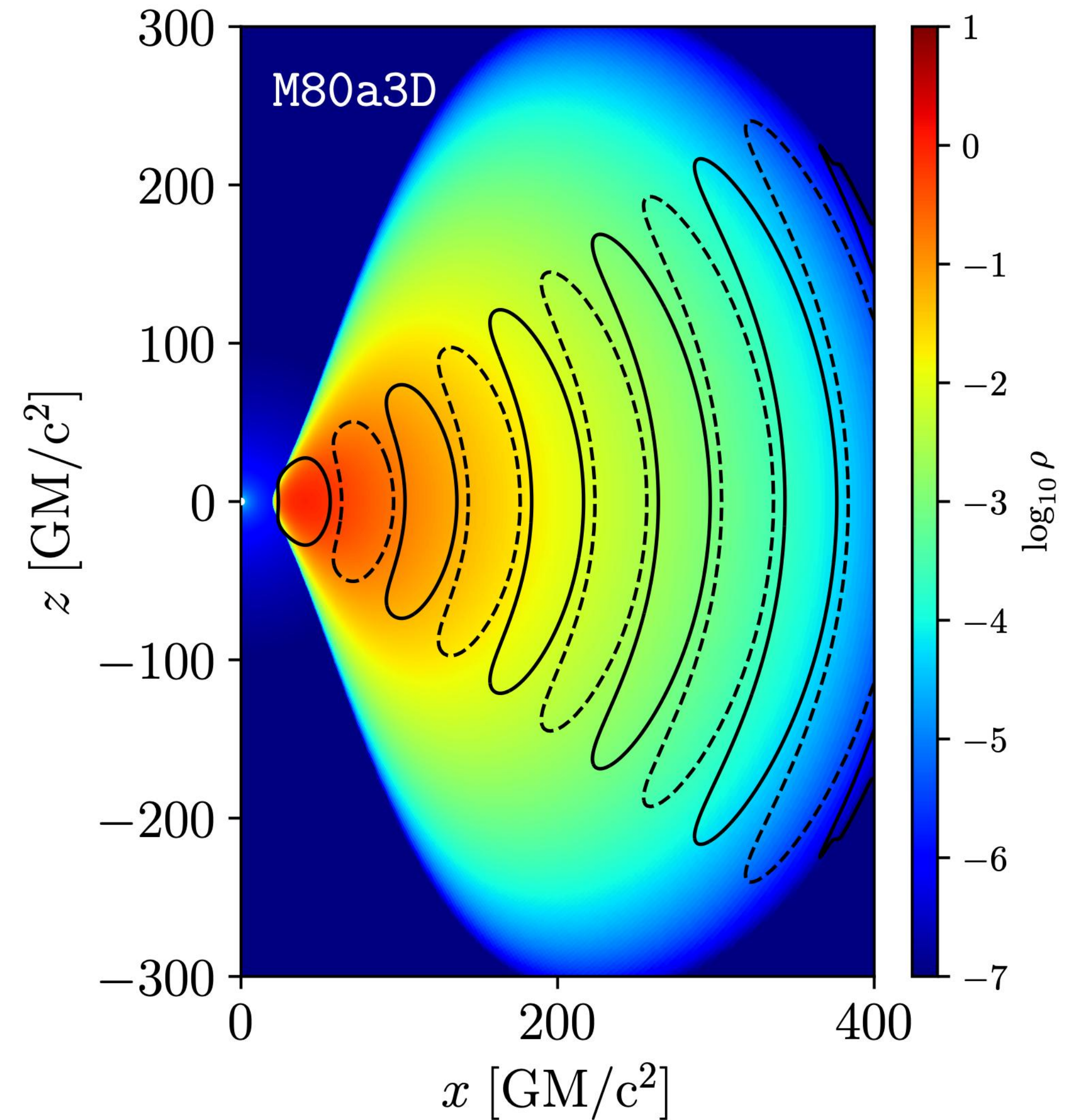
Jiang, YM, Fromm, Nathanail (2023)

Jiang, YM, Dihingia, Nathanail, Younsi, Fromm (2024)

Jiang, YM, Dihingia, et al. (2024) in prep.

GRMHD simulations with Multiple Loops

- GRMHD simulations are initiated from a geometrically thick large torus with **multiple poloidal magnetic loops** (different polarity).
- A **two-temperature module** is included to calculate electron temperature directly in GRMHD simulations.
 - turbulent & reconnection heating prescription
- Performed 2D & 3D



Electron Thermodynamics

We solve **the electron thermodynamics** during the evolution of single-MHD separately

Electron entropy equation

$$T_e \partial_\mu (\rho u^\mu s_e) = f_e Q$$

$s_e = p_e / \rho^{\Gamma_e}$: electron entropy

p_e : electron pressure, Γ_e : electron adiabatic index

f_e : fraction of the dissipative heating that goes into the electron

Q : total heating rate

- Here **neglect** energy exchange rate due to Coulomb coupling, anisotropic thermal heat flux, and radiative cooling
- Heating is provided by **the grid-scale dissipation**.

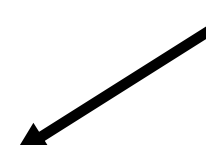
Electron thermodynamics

We solve the electron thermodynamics during the evolution of single-MHD separately

Electron entropy equation

$$\partial_\mu(\sqrt{-g}\rho u^\mu \kappa_e) = \frac{\sqrt{-g}(\Gamma_e - 1)}{\rho^{\Gamma_e - 1}} f_e Q$$

$T_e \partial_\mu(\rho u^\mu s_e) = f_e Q$

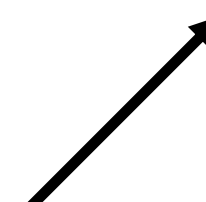


$\kappa_e \equiv \exp[(\Gamma_e - 1)s_e]$ $s_e = (\Gamma_e - 1)^{-1} \log(p_e/\rho^{\Gamma_e})$: electron entropy

Time evolution of electron entropy by heating

$$\kappa_e^{n+1} = \hat{\kappa}_e^{n+1} + \frac{\Gamma_e - 1}{\Gamma_g - 1} (\rho^{\Gamma_g - \Gamma_e} f_e)^{n+1/2} (\kappa_g - \hat{\kappa}_g)^{n+1}$$

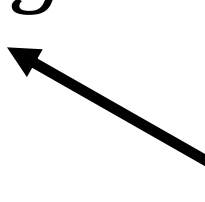
solution from entropy
conservation equation without
a source term



entropy obtained from total
energy conservation equation



entropy obtained from entropy
conservation equation



Electron Heating

- Heating is provided by grid-scale dissipation, which is related to magnetic reconnection, shock-heating, Ohmic heating, and turbulent heating.
- Here we consider two electron heating (sub-grid model):
turbulent and **magnetic reconnection**

Turbulent heating model
(e.g., Kawazura et al. 2019)

$$\frac{Q_i}{Q_e} = \frac{f_e}{1 + (\beta/15)^{-1.4} \exp(-0.1T_e/T_i)}$$
$$f_e = \frac{1}{1 + \frac{Q_i/Q_e}{35}},$$

Fitting formulae for ion-to-electron
heating rate from MHD turbulence
simulation

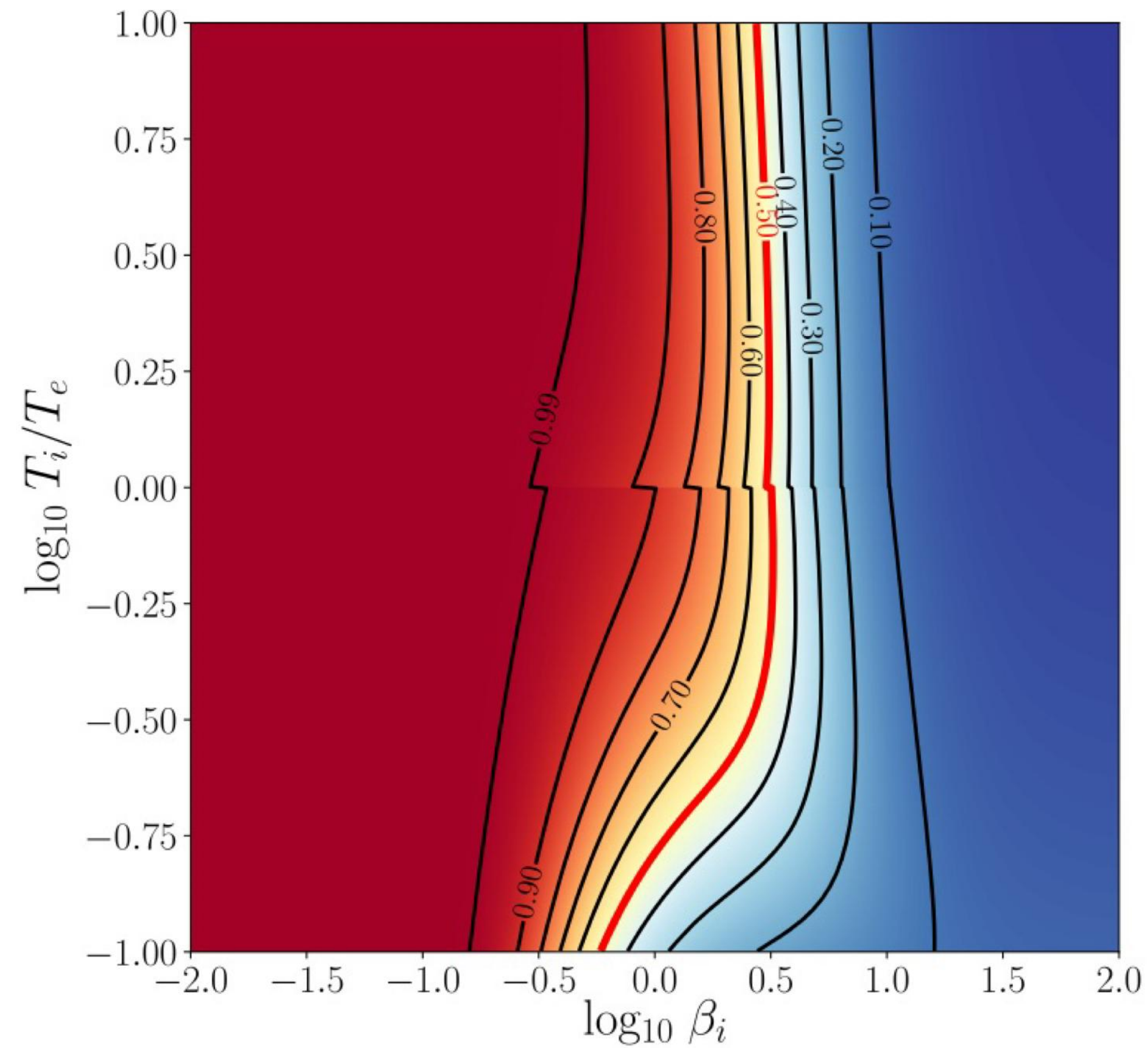
Reconnection heating model
(e.g., Rowan et al. 2017)

$$f_e = \frac{1}{2} \exp \left[\frac{-(1 - \beta/\beta_{\max})}{0.8 + \sigma_h^{0.5}} \right], \quad \begin{aligned} \beta_{\max} &= \sigma_h/4 \\ \sigma_h &= b^2/\rho h \end{aligned}$$

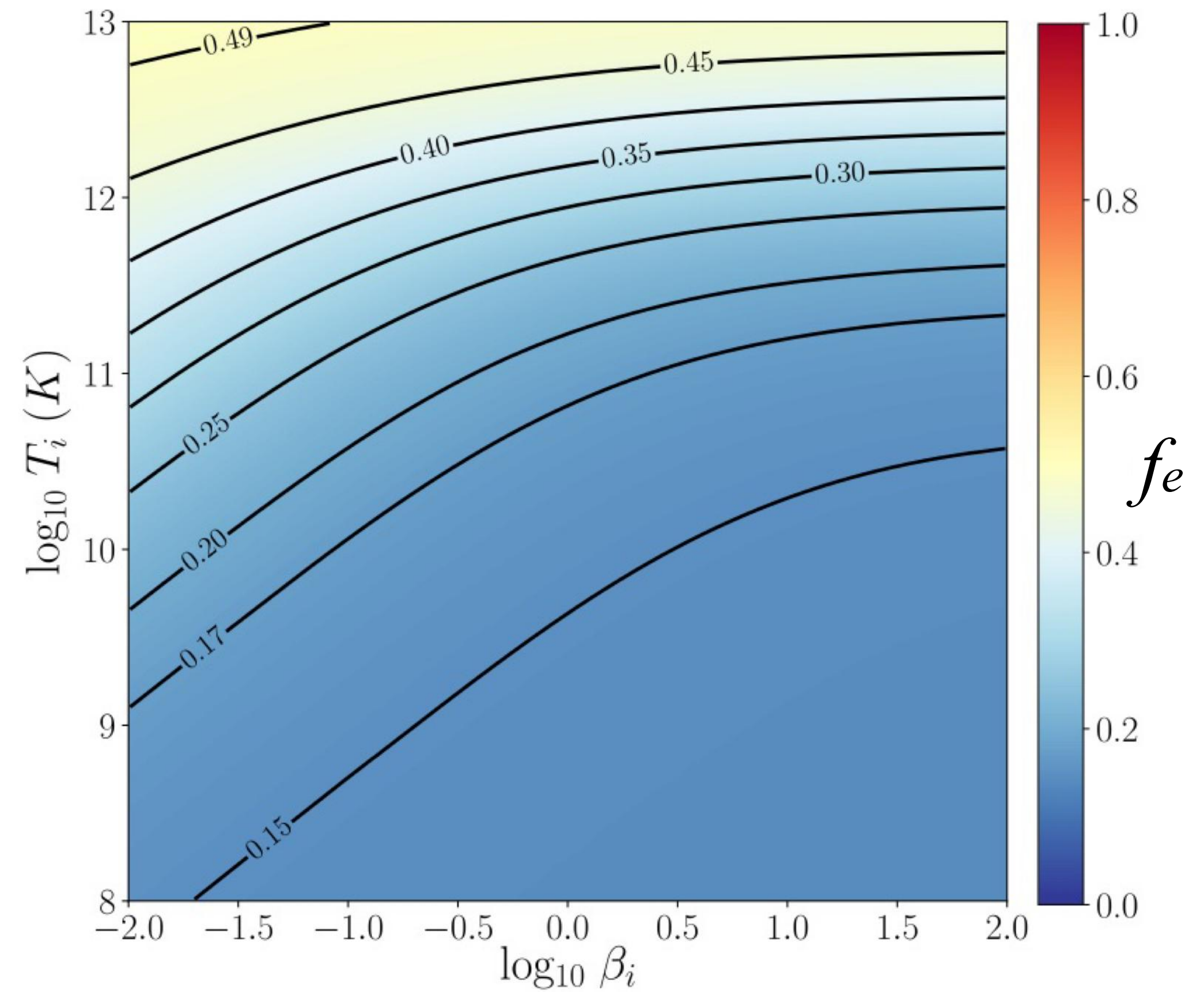
Fitting function as measured in PIC
simulations of magnetic reconnection

Electron Heating Fraction

turbulent heating



reconnection heating

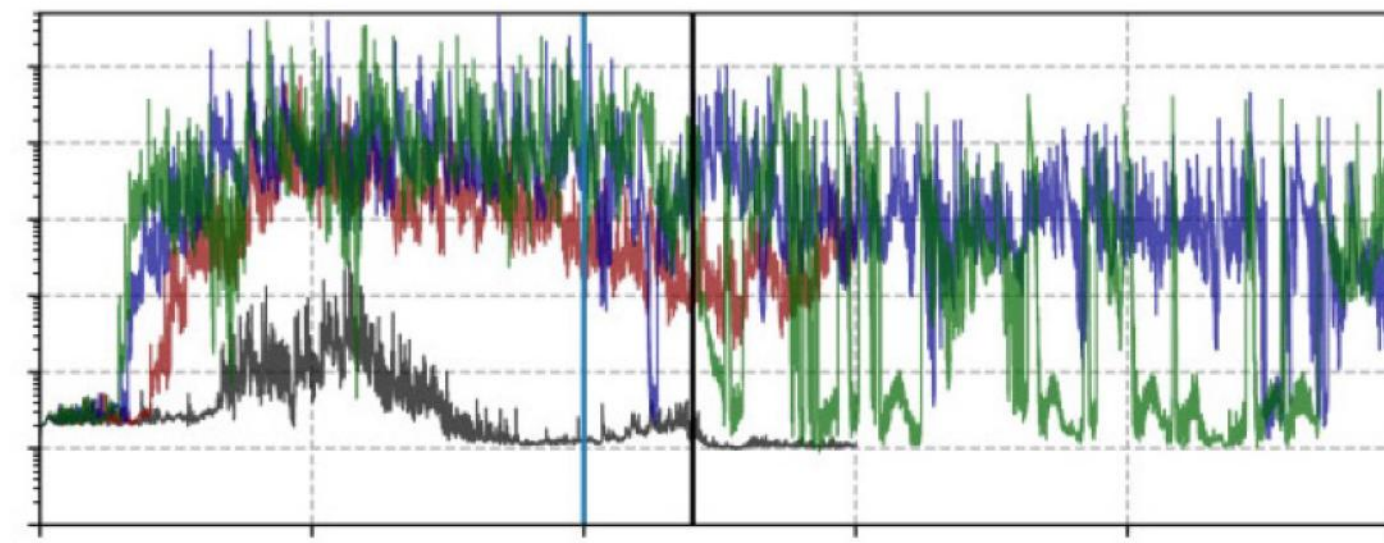
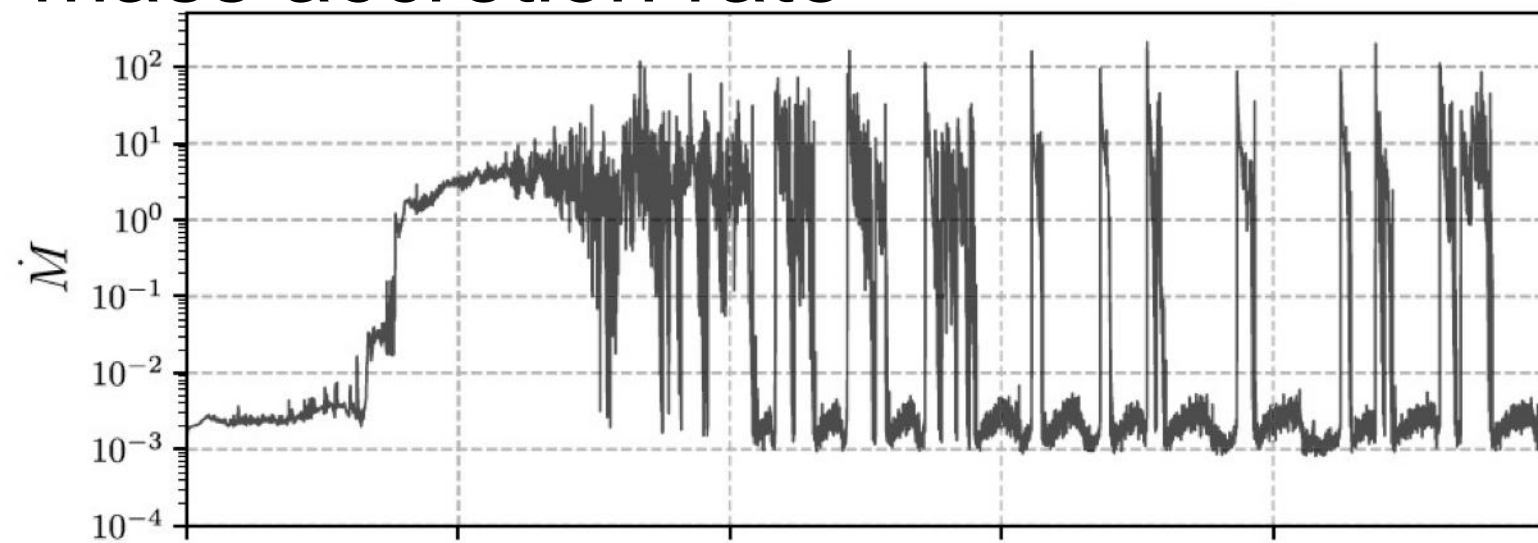


GRMHD simulations with Multiple Loops

- GRMHD simulations are initiated from a hydrostatic torus with multiple poloidal magnetic loops (different polarity).
- Two-temperature module is included to calculate electron temperature.
- Different loop length makes different accretion flow behavior (SANE-MAD transition)

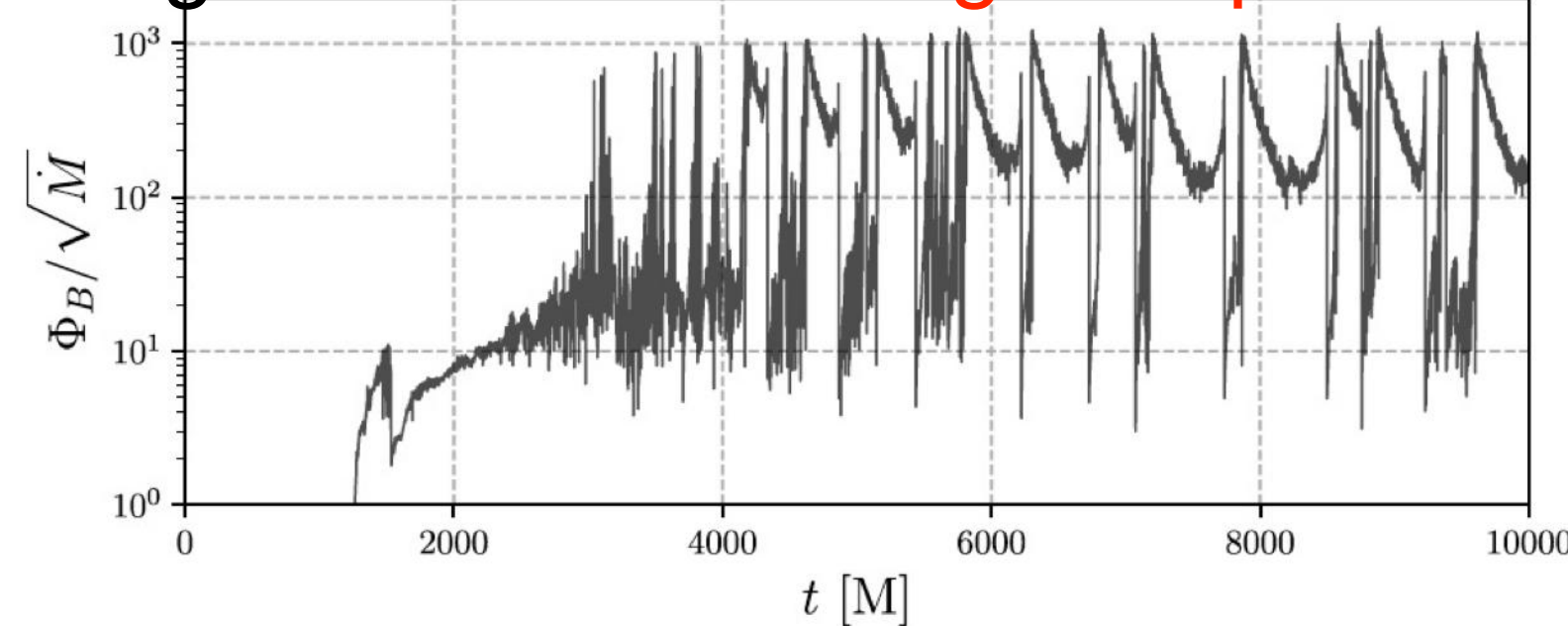
2DGRMHD

mass accretion rate

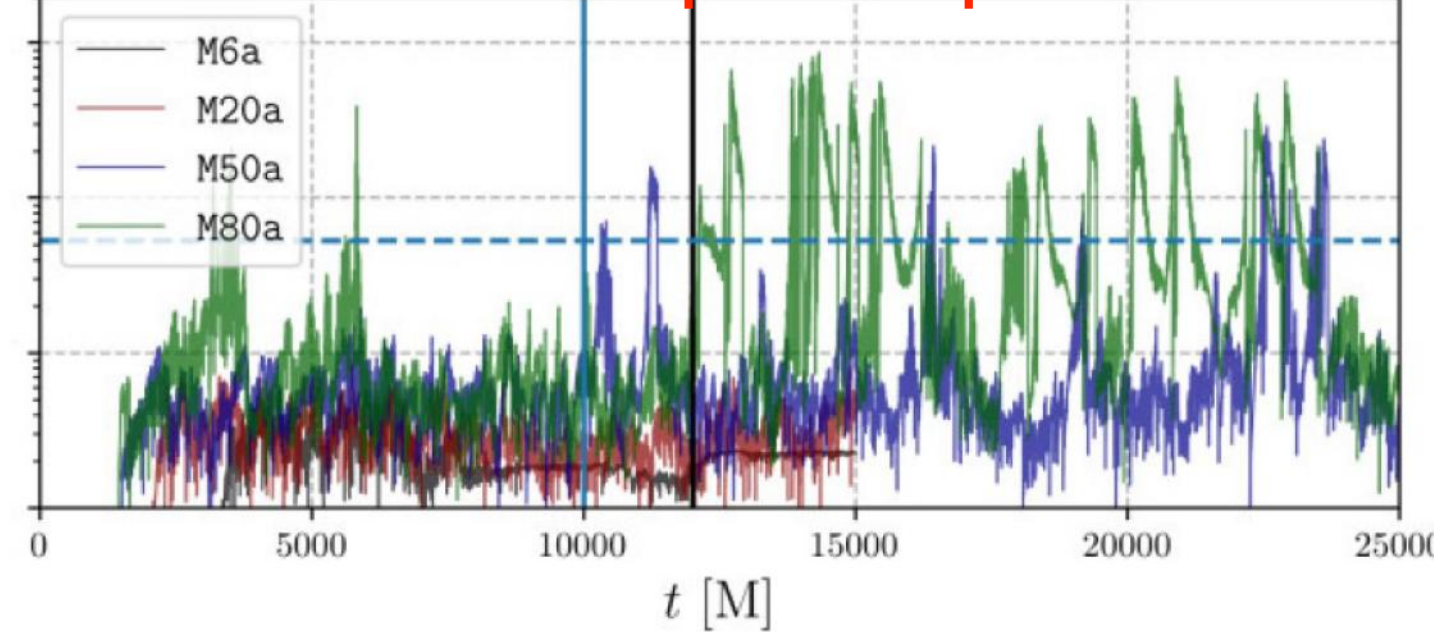


magnetic flux

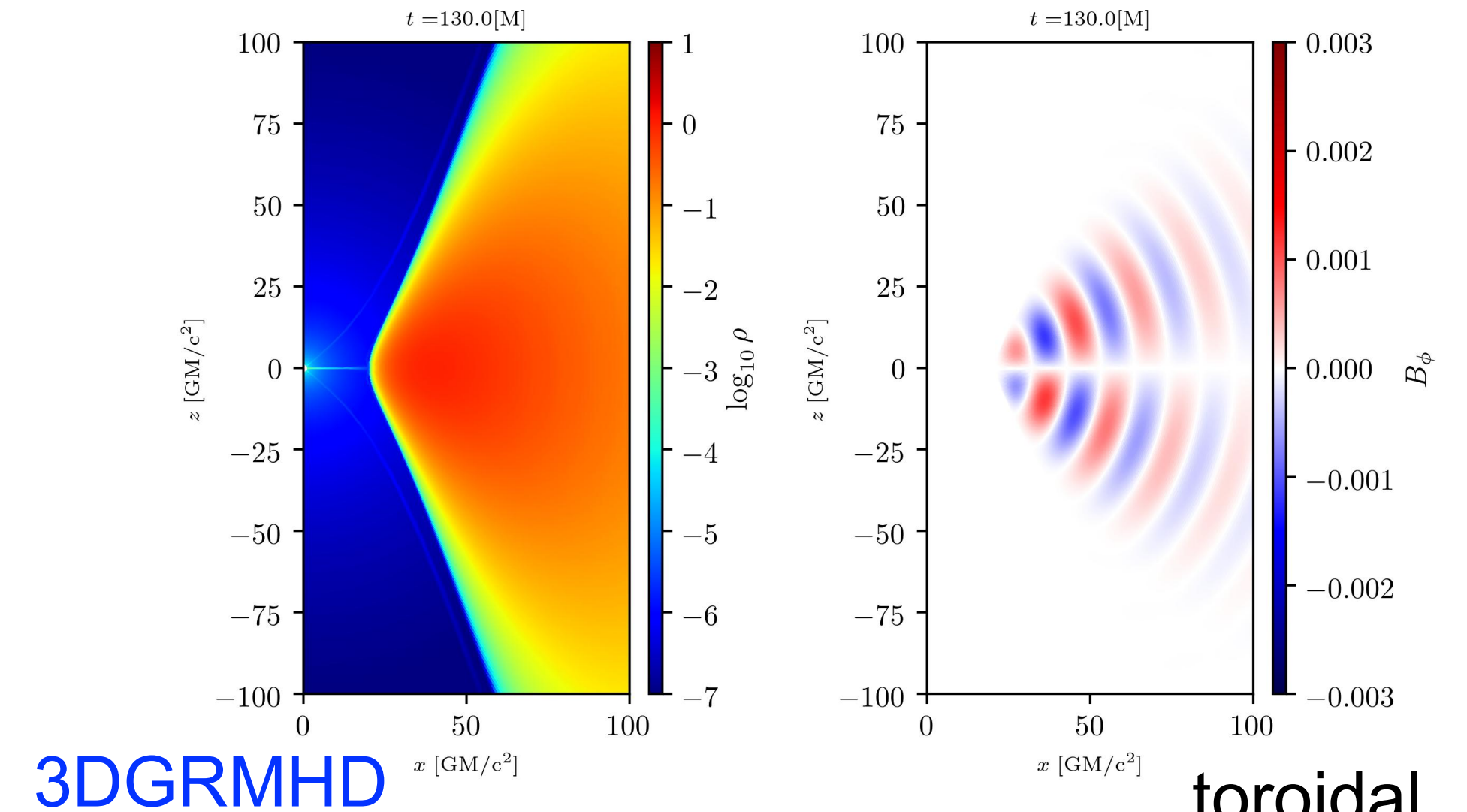
single-loop



multiple-loop

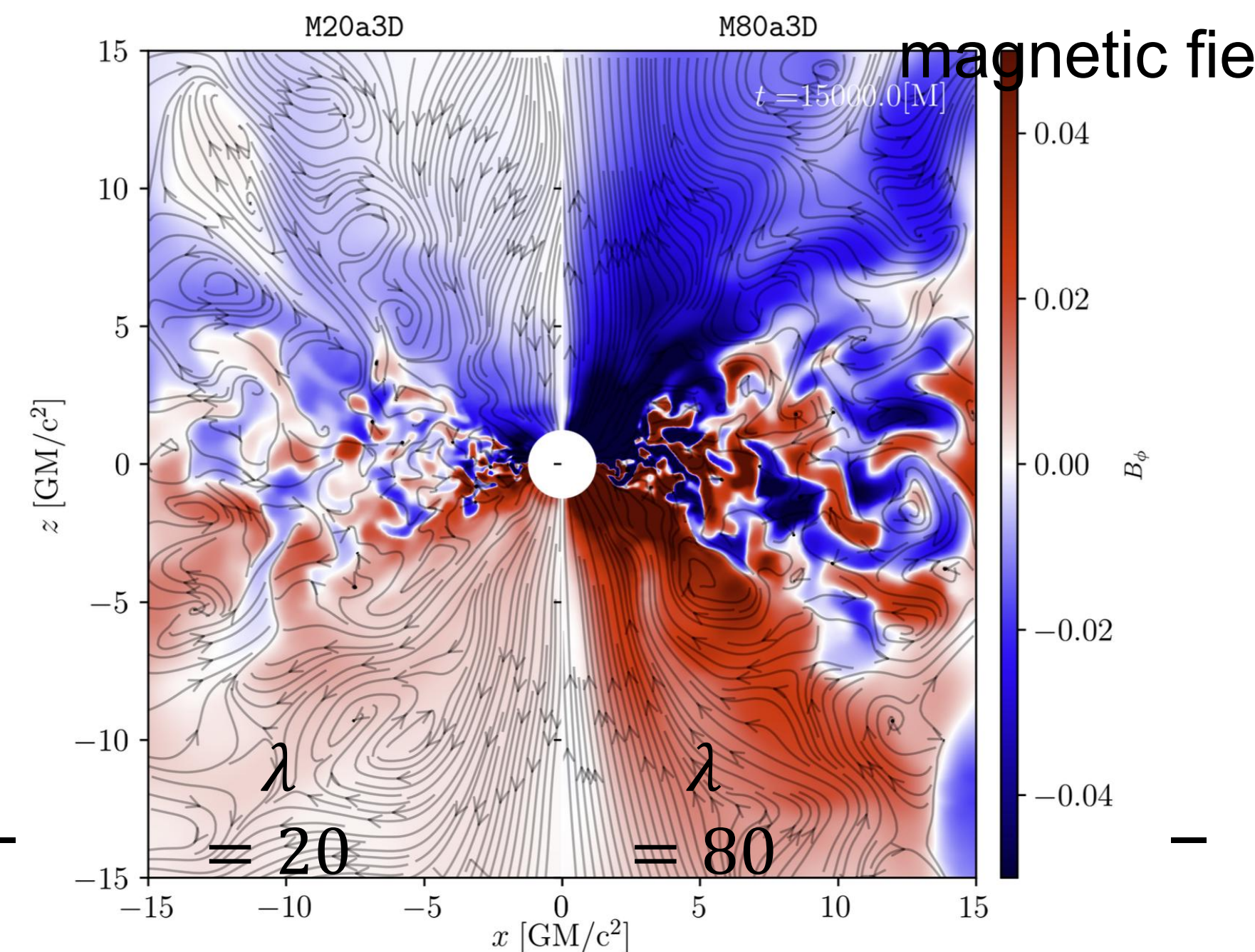


Jiang, YM, Fromm, Nathanail (23)



3DGRMHD

toroidal
magnetic field

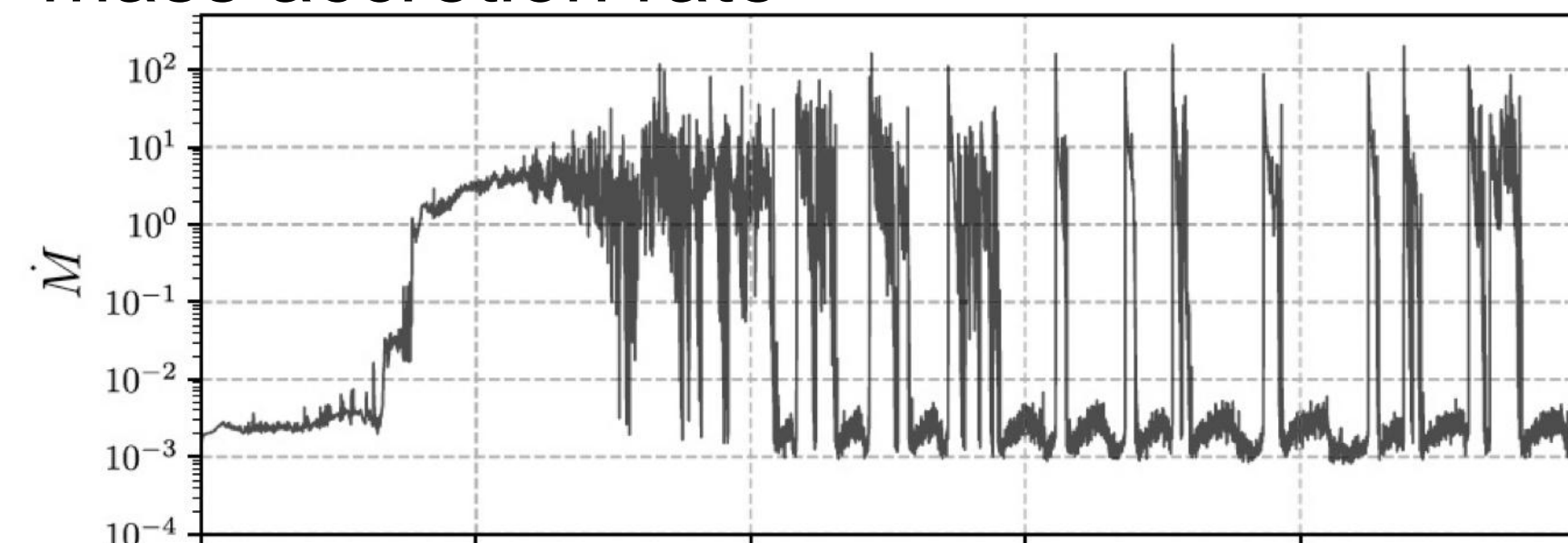


GRMHD simulations with Multiple Loops

- Different loop length makes different accretion flow behavior (**SANE-MAD transition**)

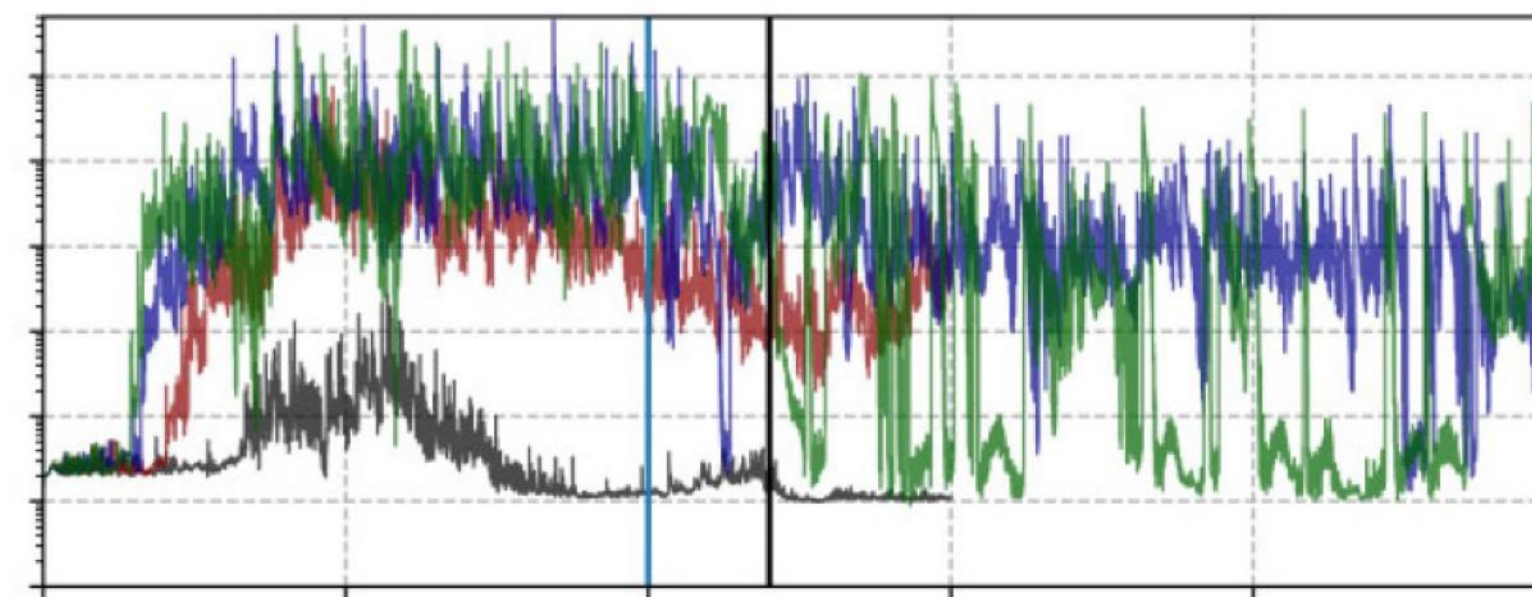
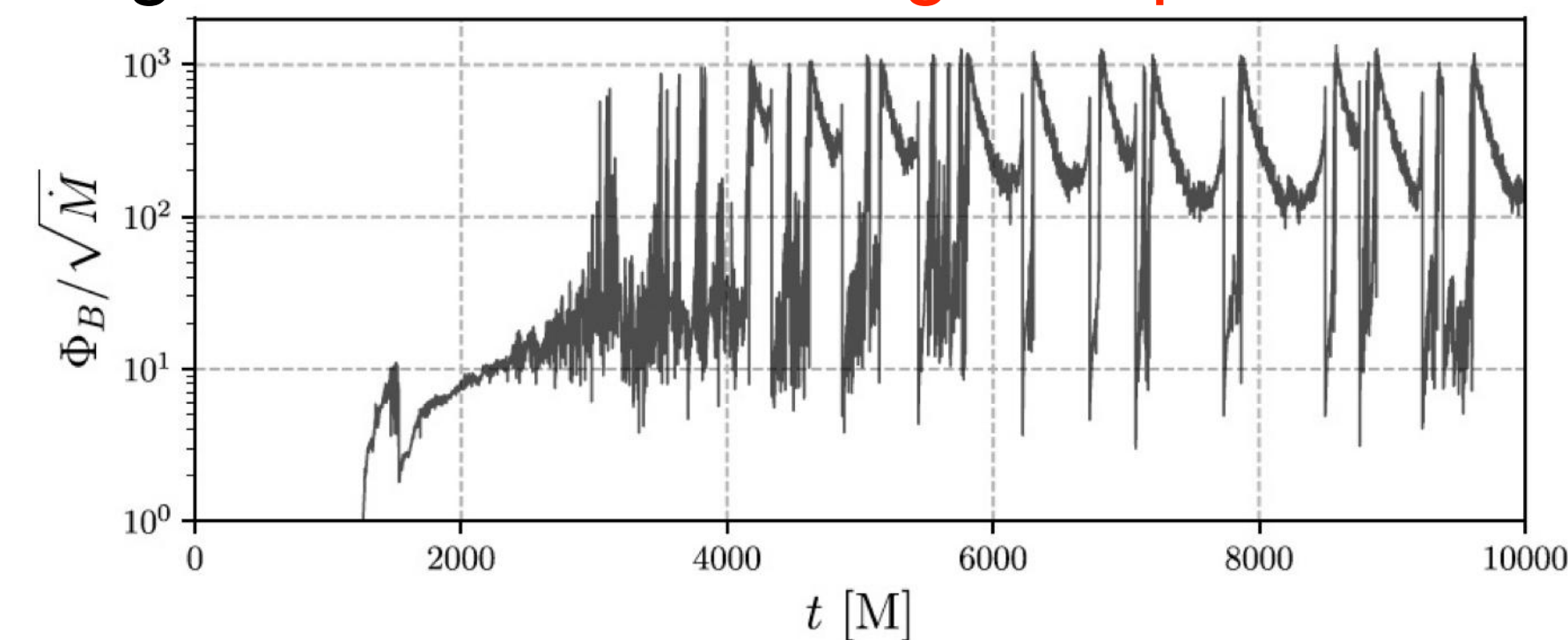
2DGRMHD

mass accretion rate

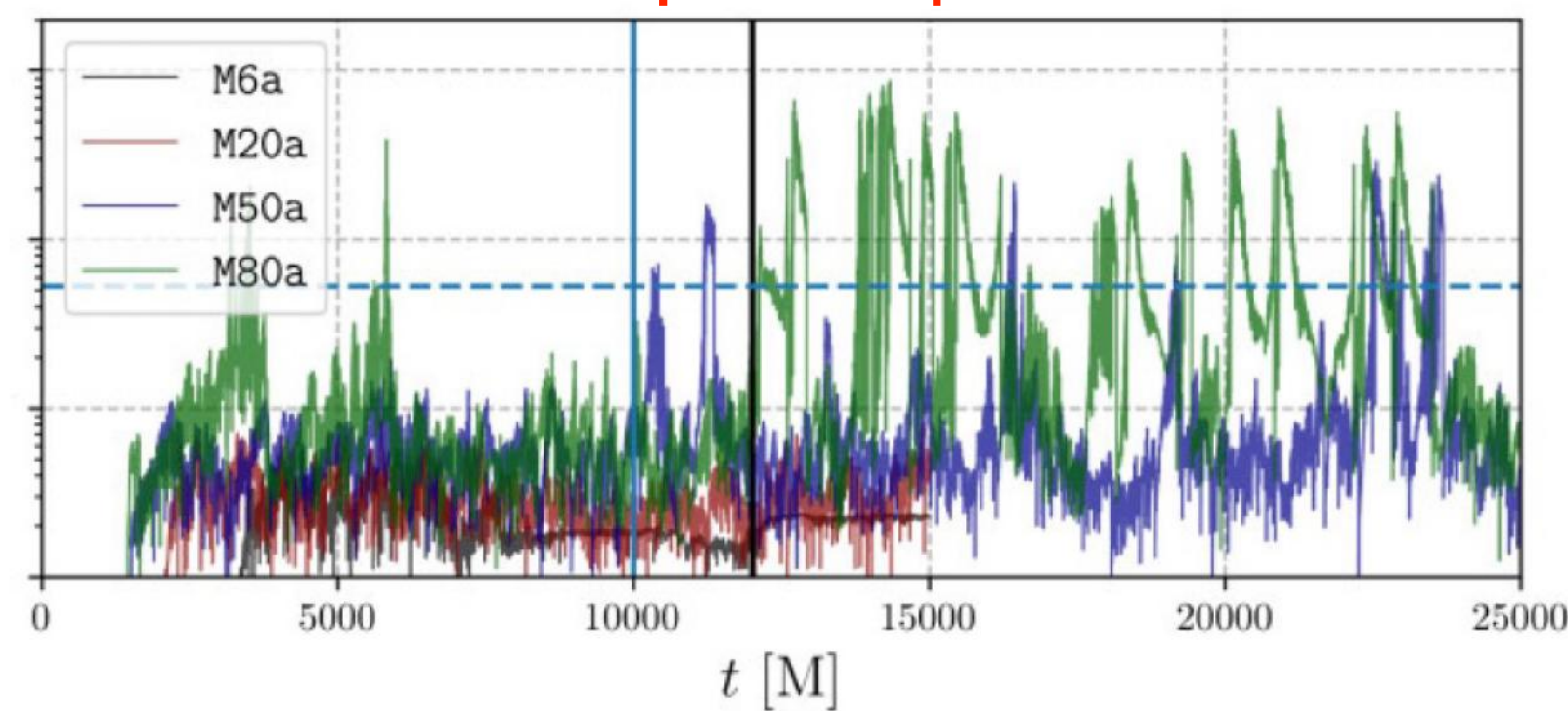


magnetic flux

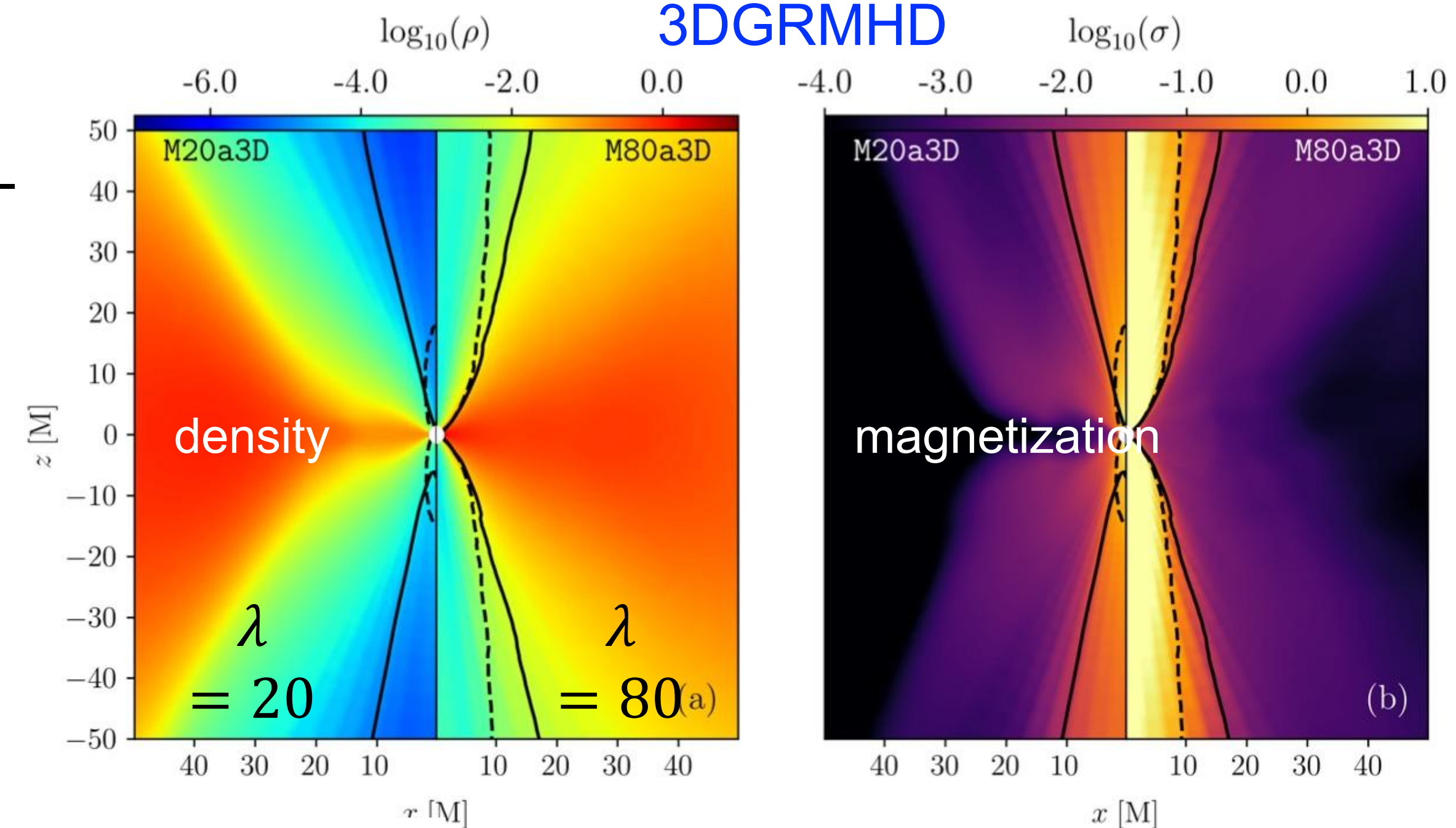
single-loop



multiple-loop



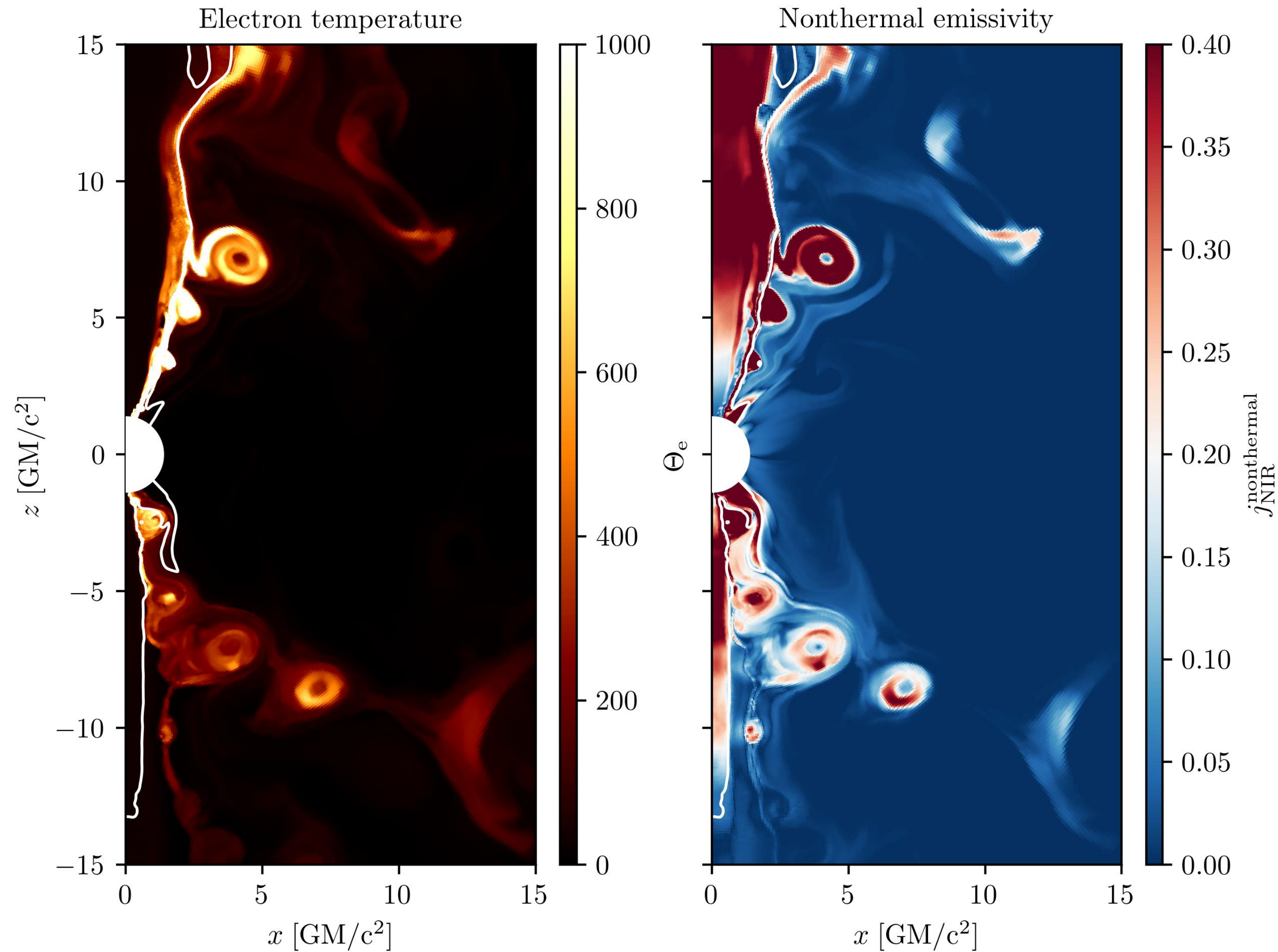
3DGRMHD



time & azimuthal
averaged images

Plasmoids in GRMHD Simulations

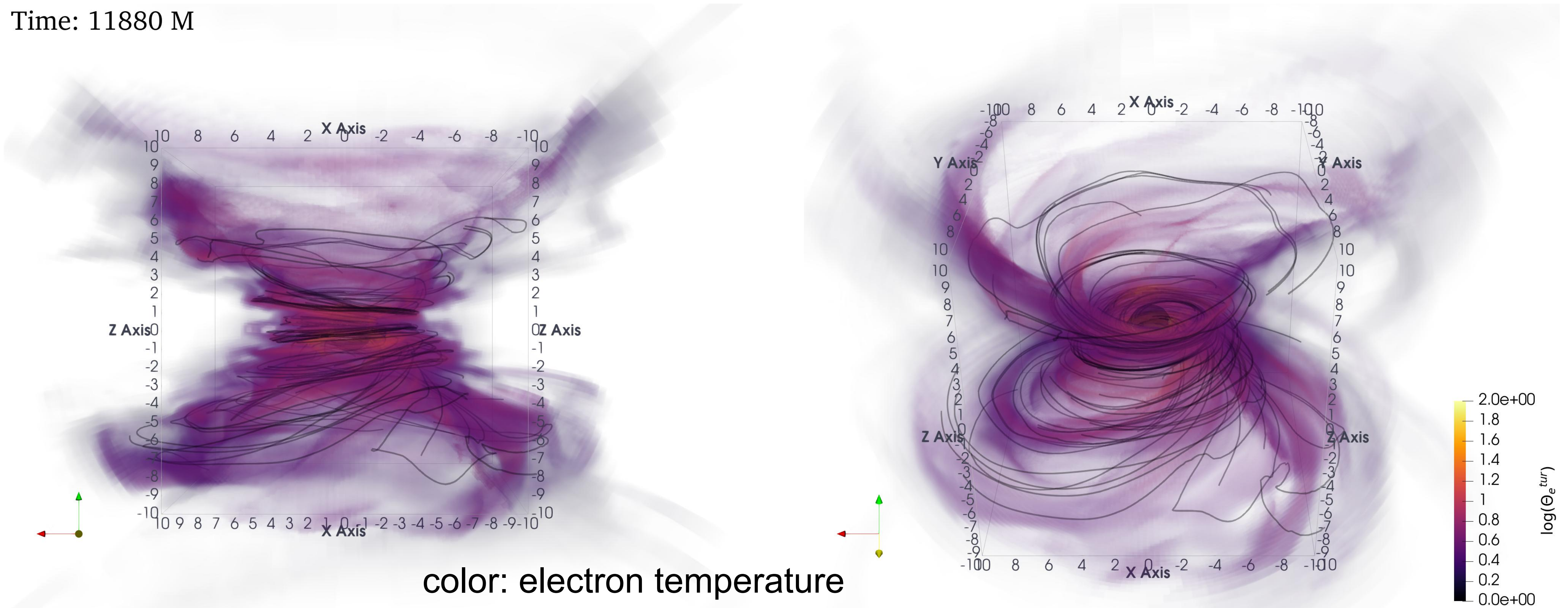
- Plasmoids and current sheets are generated via reconnection at the jet sheath.
- Plasmoids contain high electron temperature and nonthermal (near-infrared) emissivity.
- In 3D GRMHD simulations, such plasmoids correspond to emerging **magnetic flux ropes**



Magnetic Flux Rope in 3D GRMHD Simulations

Emerging magnetic flux ropes have higher electron temperature

Time: 11880 M



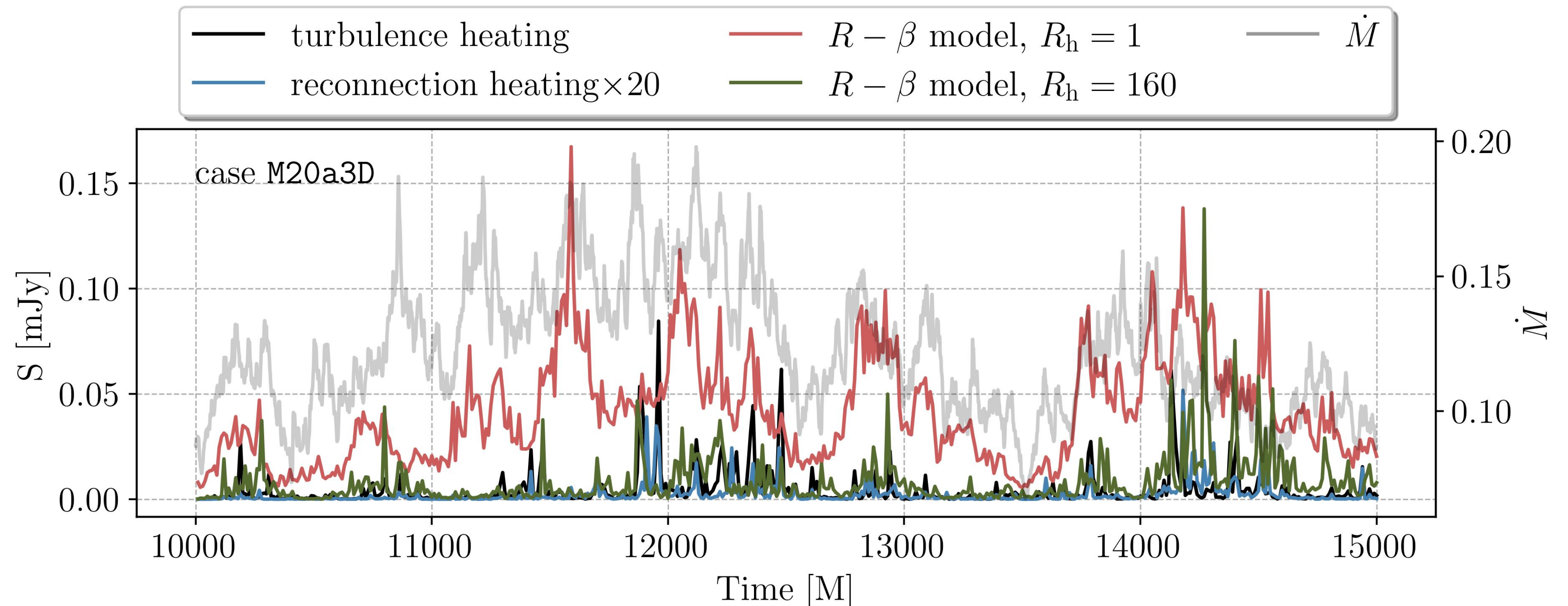
color: electron temperature
black lines: magnetic field lines

GRRT Calculations (thermal)

- Using GRRT code RAPTOR for post-process imaging calculation
 - Target for Sgr A*
 - The inclination angle is 30 degrees.
 - The accretion rate is fitted at 230 GHz with a flux of 2.5 Jy.
 - To avoid the floor value problem in GRMHD data, we cut-off a high magnetization region ($\sigma = 1$)
 - GRRT calculation uses the GRMHD data from a 5,000 M time-span in different accretion flow state
 - Consider synchrotron radiation with thermal eDF.
 - Electron temperature is given by two-temperature GRMHD directly
-

NIR Light Curve

- The strong emission spikes in the light curve is related to the flaring activities, which is related to the high electron temperature regions in the flux ropes.
- Due to the stronger dissipation in *M20a3D*, the obtained peak of the thermal NIR emission from this model is lower than observation value ($\sim 25\text{mJy}$ Abuter et al. (2020)).



GRRT Calculations (non-thermal)

- Using polarized GRRT code RAPTOR for post-process imaging calculation
 - Target for Sgr A*
 - The inclination angle is 30 degrees.
 - The accretion rate is fitted at 230 GHz with a flux of 2.5 Jy.
 - To avoid the floor value problem in GRMHD data, we cut-off a high magnetization region ($\sigma_{\text{cut}} = 1$)
 - GRRT calculation uses the GRMHD data from 10,000 to 15,000 M
 - Consider hybrid (thermal and non-thermal emission) synchrotron emission by using kappa-eDF
-

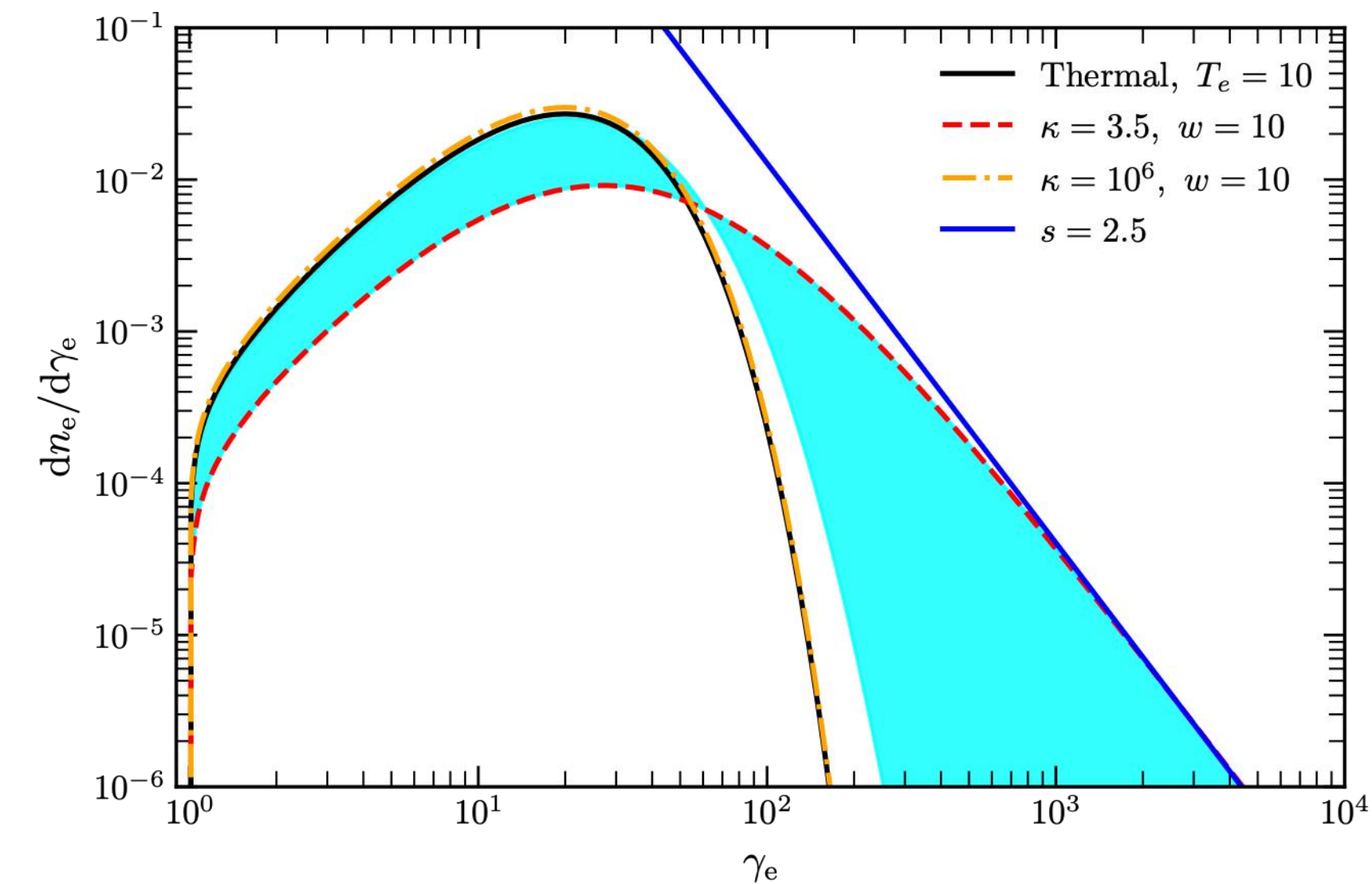
kappa distribution function (non-thermal eDF)

$$\frac{dn_e}{d\gamma} = N\gamma\sqrt{\gamma^2 - 1} \left(1 + \frac{\gamma - 1}{\kappa w}\right)^{-(\kappa+1)}$$

kappa eDF = thermal core
+ non-thermal tail

- thermal core at low values of the Lorentz factor, asymptotically turns into a power-law
- power-law index, $p = \kappa - 1$
- In the limit of $\kappa \rightarrow \infty$, the κ -distribution becomes the Maxwell–Jüttner DF
- $\kappa(\beta, \sigma) \leftarrow$ subgrid model
 - PIC sim. for [turbulence](#) (Meringolo et al. 2023)
 - $\kappa_{\text{tur}} = 2.8 + 0.2/\sqrt{\sigma} + 1.6\sigma^{-6/10}\tanh(2.25\sigma^{1/3}\beta)$

→ connect to GRMHD



kappa distribution function (non-thermal eDF)

Variable kappa eDF with efficiency function from PIC simulations

- Reconnection model (Ball et al. 2018)

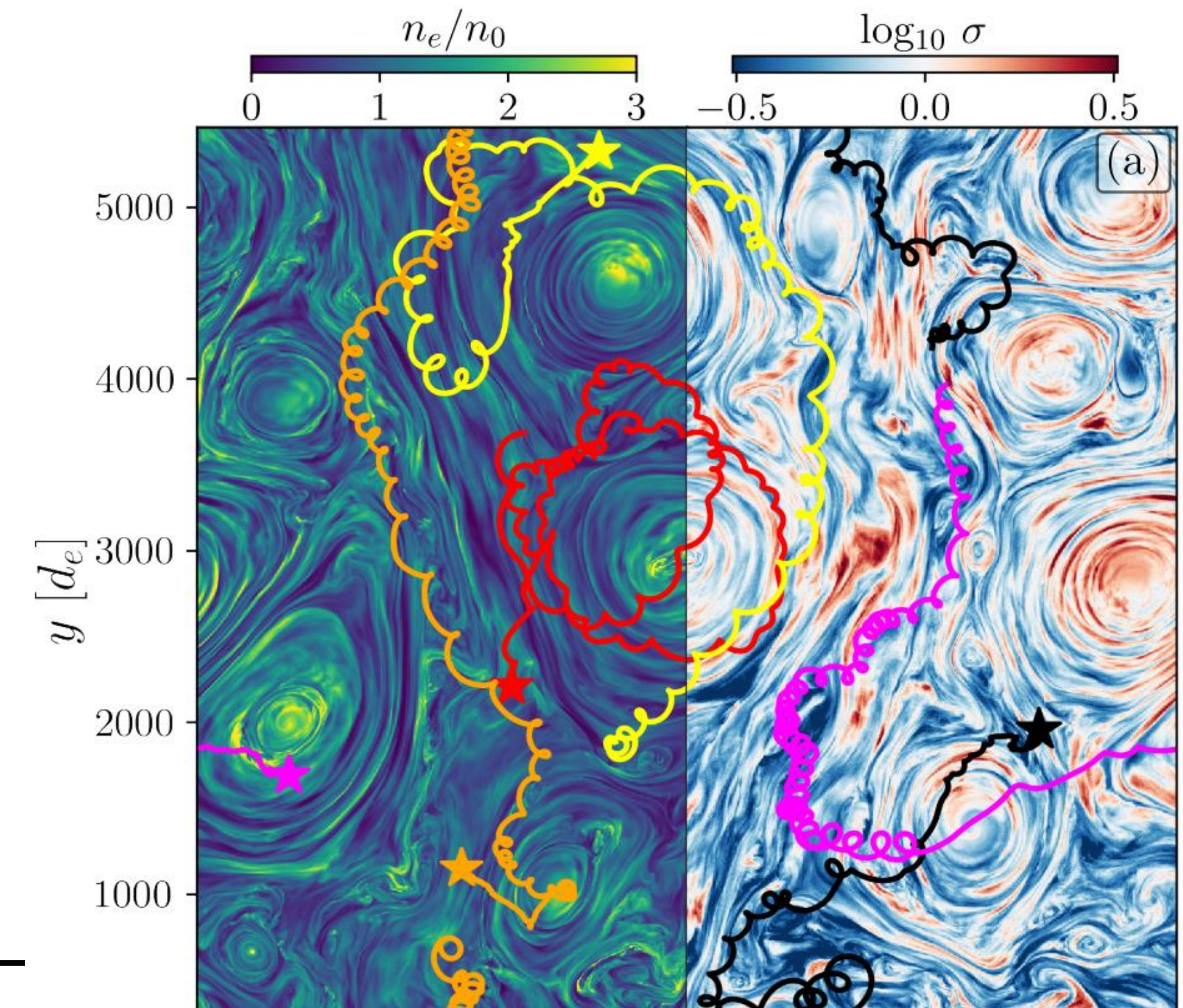
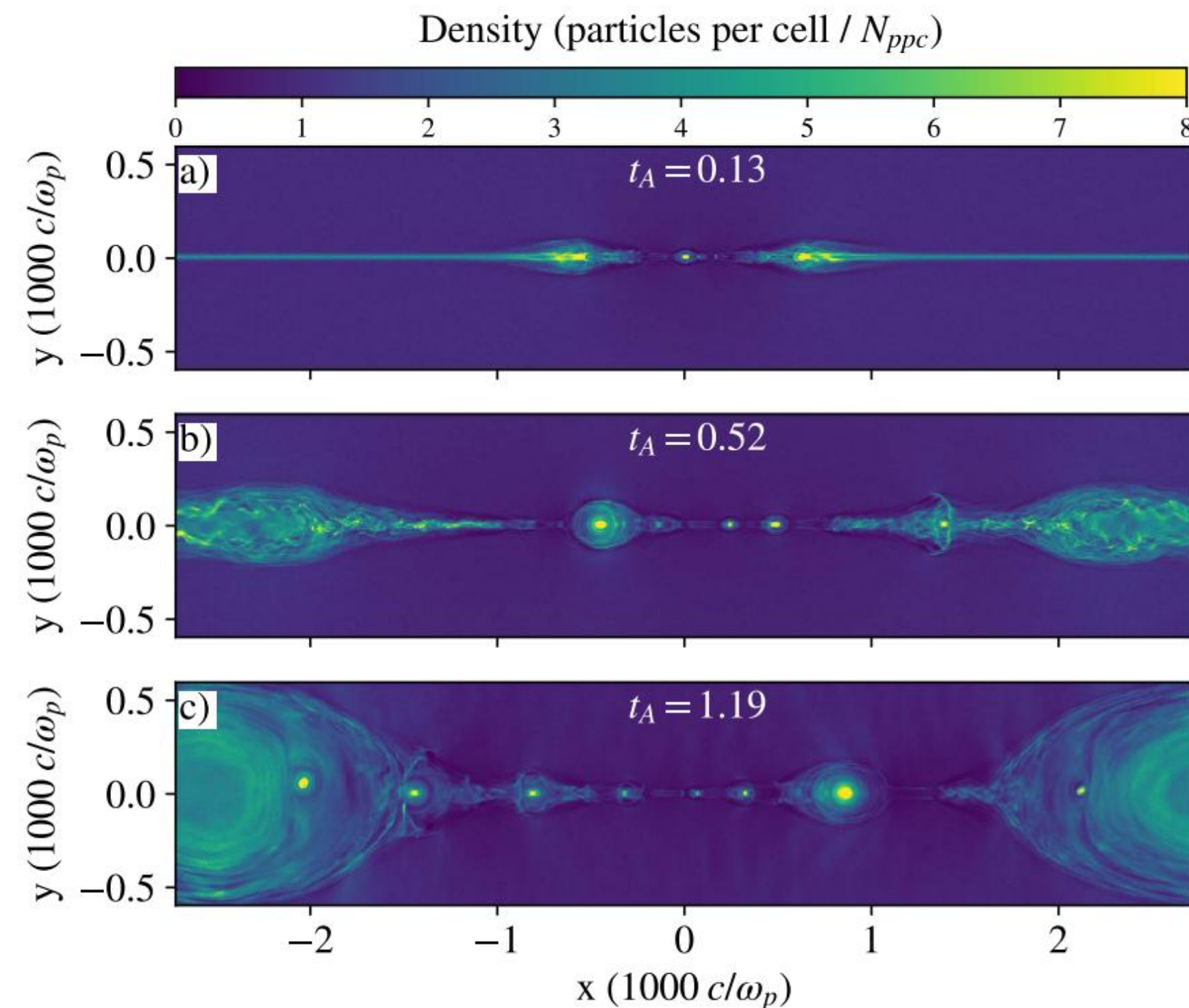
$$\kappa = 2.8 + 0.7/\sqrt{\sigma} + 3.7\sigma^{-0.19}\tanh(23.4\sigma^{0.26}\beta)$$

$$\epsilon = 1 - \frac{1}{4.2\sigma^{0.55} + 1} + 0.64\sigma^{0.07}\tanh(-68\sigma^{0.13}\beta)$$

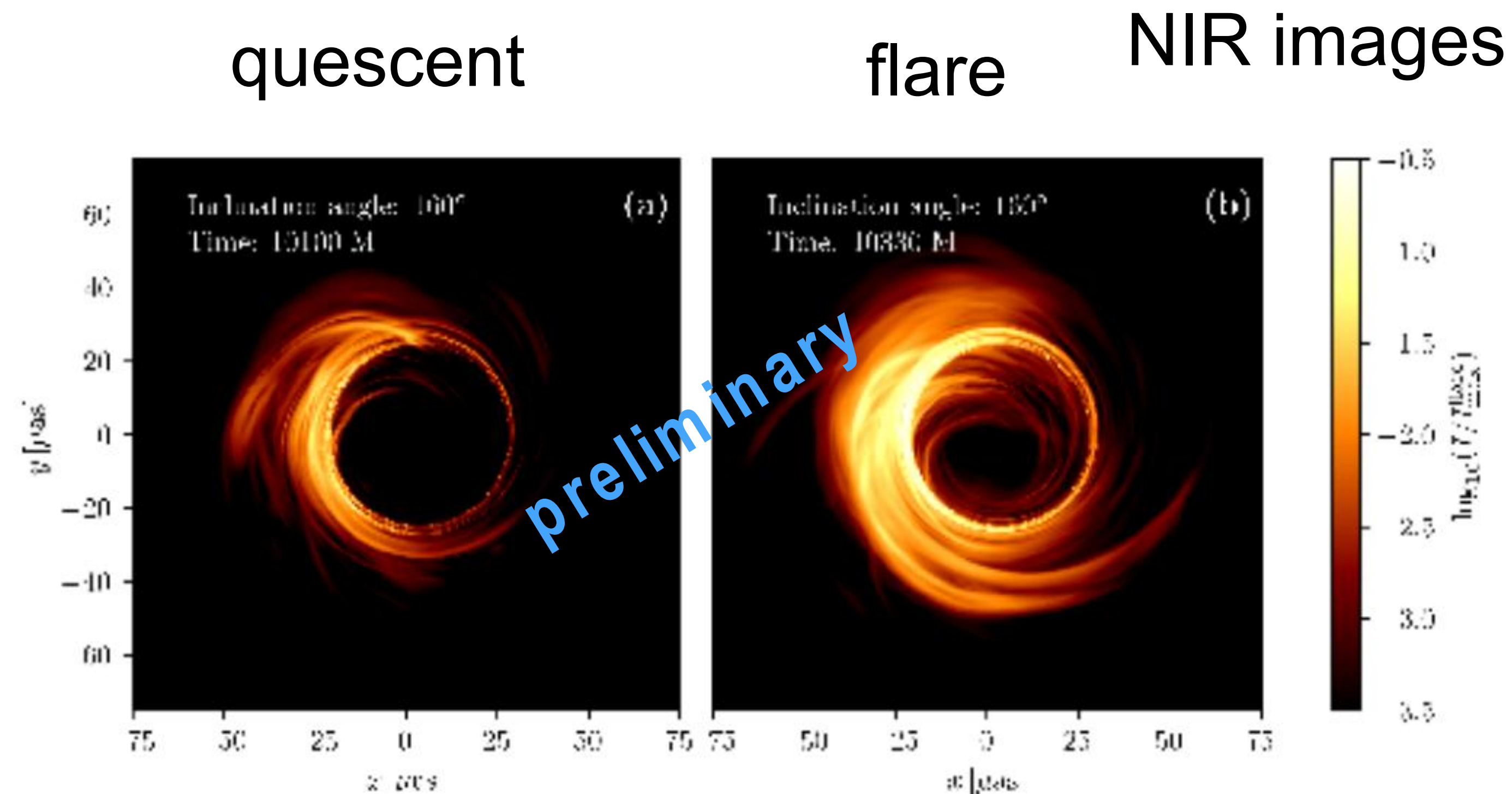
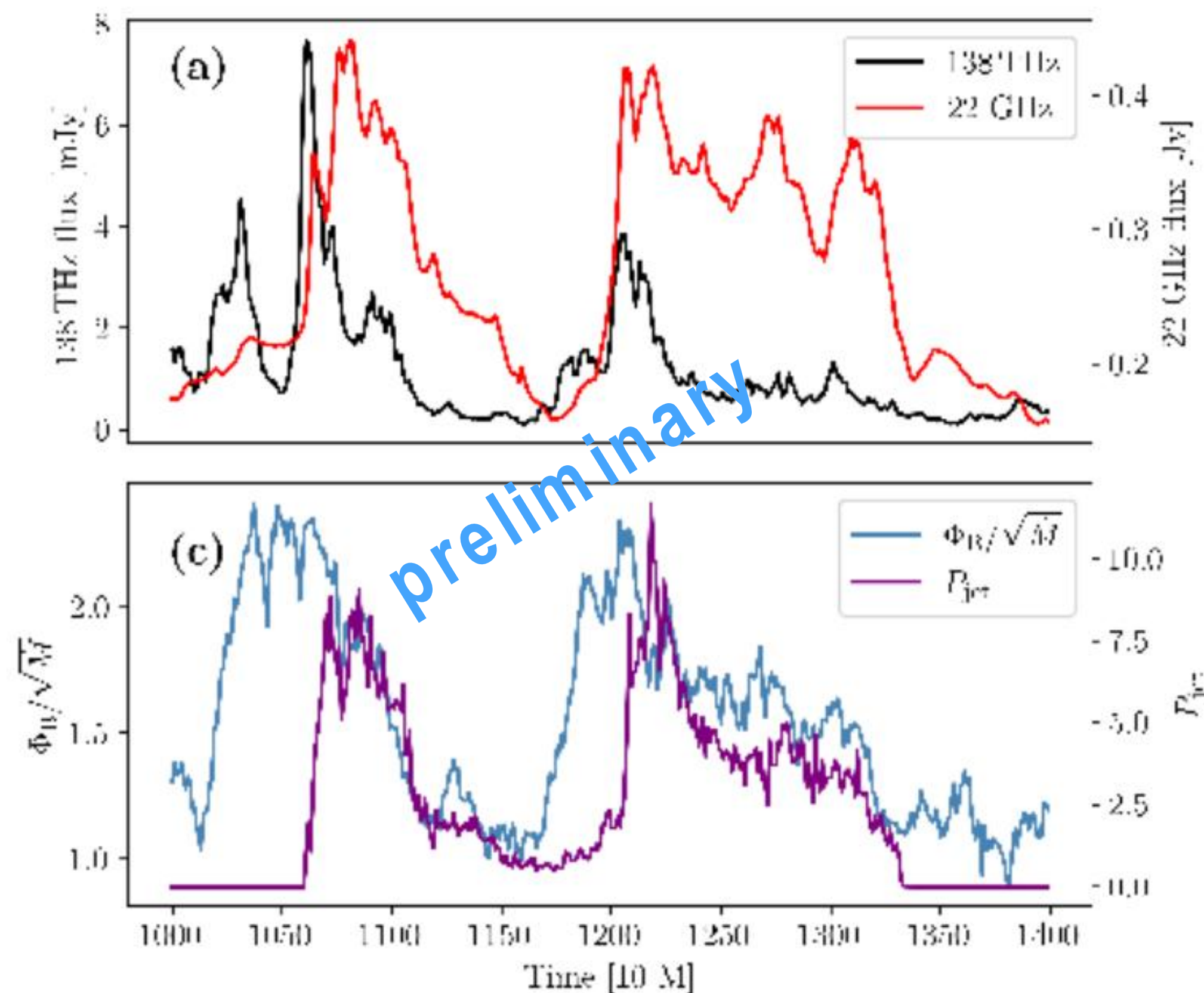
- Turbulence model (Meringolo et al. 2023)

$$\kappa = 2.8 + 0.2/\sqrt{\sigma} + 1.6\sigma^{-6/10}\tanh(2.25\sigma^{1/3}\beta)$$

$$\epsilon = 1 - \frac{0.23}{\sigma^{0.5}} + 0.5\sigma^{1/10}\tanh(-10.18\sigma^{1/10}\beta)$$



Light curves & NIR images

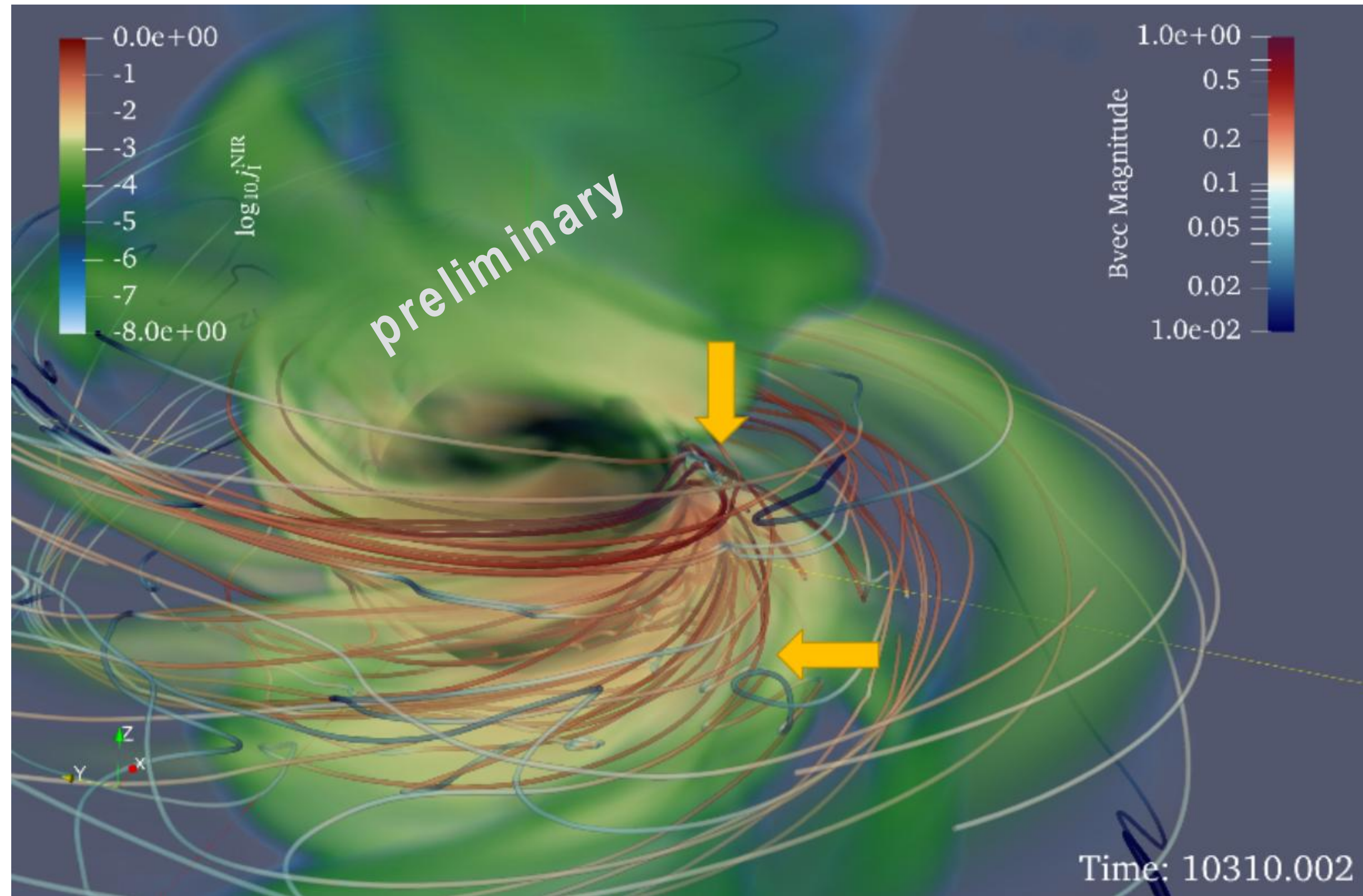


- By the contribution of non-thermal emission, we can obtain enough flux for NIR flare
- GRRT image show clear extended emission near the ring
- Flare timing at radio band is delayed => different emission region at different frequencies

NIR Emission Region

Color: NIR
emissivity
Line: Magnetic field

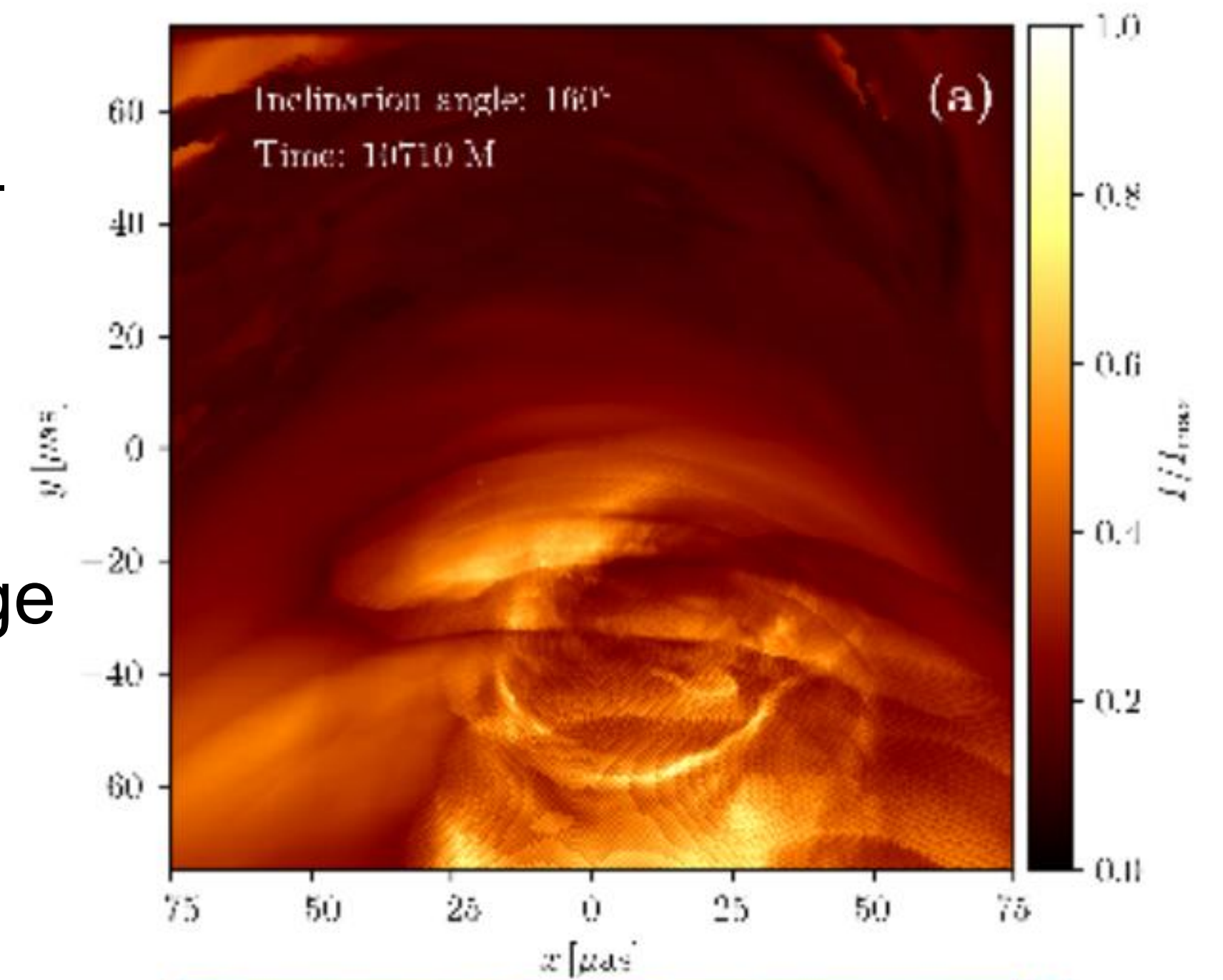
- Magnetic flux has relatively high emissivity.
- Magnetic reconnection happens at the root of magnetic flux => NIR flare



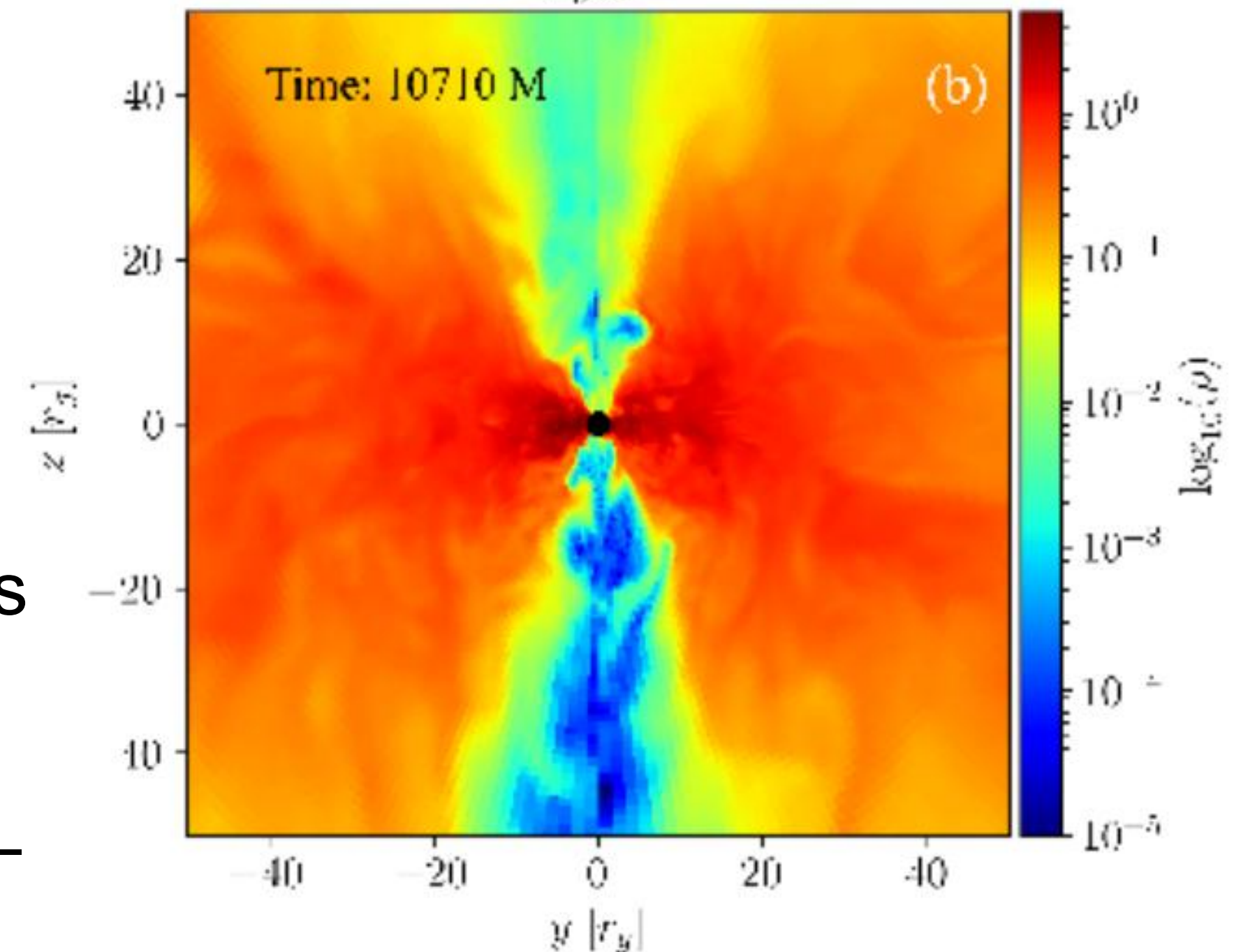
Radio flare

- 22GHz image is mostly optically thick => do not see clear ring-like emission
- 22GHz flare is correlated with Jet power activity
- When jet is formed, the jet spine region becomes low-density and optically thin.
- Emission from jet base = 22GHz flare

22GHz image



GRMHD
simulations
(density)



Summary

- Hotspot model can explain observational feature seen in Sgr A* flare, however physical mechanism of hotspot is still unknown.
 - GRMHD simulations with single magnetic loop configuration shows the ejection of flux bundles on equatorial plane during MAD phase that circulate around central BH (potential properties for hotspot)
 - In GRRT images, we see a radio flare and polarization QU loops although QU loops show at the decaying phase of radio flare
 - Multi-loop magnetic configuration generates multiple flux ropes which is another potential model for the flaring activity of Sgr A*.
 - From the contribution of non-thermal emission, we reproduce NIR flare and see time delay between NIR and radio flares
-